

Analysis of weak-interaction effects in high-transverse-momentum hadron-hadron collisions*

Ephraim Fischbach and George W. Look†

Physics Department, Purdue University, West Lafayette, Indiana 47907

(Received 8 April 1977)

Parity-violating (pv) weak effects in inclusive hadron-hadron scattering processes such as $pp \rightarrow \pi^+ X$ and $pp \rightarrow \Lambda X$ are studied in the framework of the parton model. Such effects arise from the coherent interference of the strong and weak parton-parton scattering amplitudes, and manifest themselves experimentally through a difference in the cross sections for protons incident with initial \pm helicity, or through a longitudinal polarization of the outgoing Λ produced by an unpolarized beam. Results for the corresponding pv parameters \mathcal{Q} and \mathcal{P} are presented assuming a variety of weak-interaction models. For the strong parton-parton interaction we use the recently introduced effective-gluon model. A detailed discussion is given of phases in the weak and strong interactions and of the strong-weak relative phase in various models. It is shown that both $|\mathcal{Q}|$ and $|\mathcal{P}|$ increase with increasing \sqrt{s} and $x_1 = 2p_1/\sqrt{s}$, where \sqrt{s} is the center-of-momentum energy and p_1 is the transverse momentum of the inclusively produced π^+ or Λ . For $\sqrt{s} = 20$ GeV and $x_1 = 0.6$, $|\mathcal{Q}|$ and $|\mathcal{P}|$ can be as large as 10^{-3} – 10^{-4} in some models, which may make such effects detectable in future experiments. In other models \mathcal{Q} and \mathcal{P} can actually vanish identically for certain values of \sqrt{s} and x_1 due to cancellation among the individual quark contributions. It is noted that, for a given weak-interaction model, the dependence of \mathcal{Q} and \mathcal{P} on x_1 and \sqrt{s} is different in the effective-gluon and constituent-interchange models, and hence weak effects can be used to discriminate among models of the strong interaction. A discussion is also given of various experimental problems associated with measuring \mathcal{Q} and \mathcal{P} .

I. INTRODUCTION

It is widely believed at the present time that hadrons behave in certain respects as if they were composed of still more elementary constituents called partons, such as spin- $\frac{1}{2}$ quarks and spin-1 vector gluons. Although these constituents have never been seen in isolation, the circumstantial evidence for their existence is in many ways quite compelling. Thus, for example, the spectrum of ordinary hadrons suggests that the low-lying mesons are $q\bar{q}$ bound states, where q denotes one of the quarks u , d , or s , while the baryons are qqq states.¹ Furthermore, the spectrum of the new mesons J/ψ , ψ' , etc. is in qualitative agreement with the charmonium model² in which these particles are treated as charm-anticharm bound states. Perhaps the most convincing evidence in favor of the parton picture comes from deep-inelastic electron and neutrino scattering^{3,4} in which the electron or neutrino can be pictured as scattering from more or less elementary spin- $\frac{1}{2}$ quarks.

If the parton picture is indeed correct then one of the first problems that one must confront is that of the interaction of the partons among themselves. Although parton-parton scattering cannot be studied directly (e.g., the way proton-proton scattering can), it is accessible indirectly through a study of scatterings in which particles appear with large transverse momenta (p_\perp)—if we assume that the interaction is dominated by parton-parton

or parton-hadron scattering subprocesses.

Experimental support for the parton picture of hadron-hadron scattering comes from the observation that in hadron-hadron interactions at high energies the number of secondary particles produced with large momenta transverse to the direction of the incident particles is larger than that expected from the typical nonparton picture. It is known, for example, that regardless of the nature of the incident particles, the average value of p_\perp for the particles emerging from the collision is⁵

$$\langle p_\perp \rangle \approx 300\text{--}400 \text{ MeV}/c. \quad (1.1)$$

The reason for the small value of $\langle p_\perp \rangle$ is that the differential cross sections for producing secondary particles with large p_\perp fall dramatically as p_\perp increases. In elastic scattering, for example, the differential cross sections are diffractive for small values of the center-of-momentum (c.m.) scattering angle $\theta_{\text{c.m.}}$ with a large peak at $t=0$, where $-t$ is the square of the four-momentum in the collision. Near the forward direction the differential cross section for pp scattering falls as⁶

$$d\sigma/d\Omega \propto e^{13t}, \quad (1.2)$$

for $950 \text{ GeV}^2 \leq s \leq 2820 \text{ GeV}^2$, where \sqrt{s} is the c.m. energy. However, near $\theta_{\text{c.m.}} = 90^\circ$ this exponential behavior gives way to a power law in the momentum transfer. The rise of the elastic cross section in this kinematic region above the value expected from an extrapolation of the exponential behavior seen at small p_\perp suggests that a new mech-

anism is being seen in elastic scattering at large p_{\perp} . A similar behavior is also observed for the inelastic inclusive cross sections $pp \rightarrow cX$, where c is a hadron and X is anything. For $p_{\perp} \lesssim 1$ GeV/ c the invariant cross sections $E_c d\sigma/d^3p_c$ also fall exponentially with increasing p_{\perp} , as indicated by the example of pion production where⁷

$$E_{\pi} d\sigma/d^3p_{\pi} \propto e^{-a p_{\perp}}, \quad a \cong 6-8 \text{ (GeV}/c)^{-1}. \quad (1.3)$$

The low- p_{\perp} cross sections join smoothly onto those for $p_{\perp} > 2$ GeV/ c which are experimentally observed to decrease (more slowly) as an inverse power of p_{\perp} :

$$E_c d\sigma/d^3p_c \sim p_{\perp}^{-n} F'(x_{\perp} = 2p_{\perp}/\sqrt{s}), \quad p_{\perp} > 1-2 \text{ GeV}/c. \quad (1.4)$$

The value of the exponent n varies from 6 to 12 depending upon the particle c and the values of s and x_{\perp} , and F' is an unspecified function of x_{\perp} .

As we have already noted, the transition from an exponential to a power-law falloff of elastic and inelastic differential cross sections with increasing p_{\perp} suggests the presence of a new scattering mechanism at high p_{\perp} . The observation of a larger than expected number of particles in the kinematic region populated by high- l events is reminiscent of Rutherford scattering and hence suggests that one may be observing the hard scattering of constituents of the proton. This suggestion motivates the study of high- p_{\perp} scattering at high energy as a probe of the interaction of these constituents among themselves.

Although high-energy differential cross sections decrease less rapidly with increasing p_{\perp} , they are nonetheless quite small at high p_{\perp} . It was pointed out in Refs. 8 and 9 that strong-interaction differential cross sections have already been measured down to levels that are characteristic of weak processes. Thus at the highest values of p_{\perp} one might expect to see parity-violating (pv) effects arising from the interference of the strong and weak parton-parton scattering amplitudes. Such effects would be manifested through non-vanishing values of the asymmetry parameters \mathcal{Q} and \mathcal{P} ,

$$\mathcal{Q} = \frac{d\sigma^+ - d\sigma^-}{d\sigma^+ + d\sigma^-}, \quad (1.5)$$

$$\mathcal{P} = \frac{d\sigma_+ - d\sigma_-}{d\sigma_+ + d\sigma_-}. \quad (1.6)$$

In Eq. (1.5) $d\sigma^{\pm}$ represent the differential cross sections (either $d\sigma^{\pm}/d\Omega$ for elastic scattering or $E d\sigma^{\pm}/d^3p$ for single-particle inclusive scattering) for pp scattering where the incident proton has \pm helicity. In Eq. (1.6) $d\sigma_{\pm}$ similarly denote the cross sections for producing a high-energy baryon in a

state of \pm helicity from an unpolarized incident proton beam. Clearly, any dependence of the differential cross section on helicity leading to non-vanishing values of \mathcal{Q} or \mathcal{P} is a parity-violating effect directly attributable to the weak interaction.

Parity violation in high-energy hadron-hadron scattering has been considered previously by a number of authors.¹⁰⁻¹⁸ Following a suggestion by Henley and Krejs^{10,11} that weak effects could be enhanced at high p_{\perp} , Fischbach and Look^{8,9} calculated \mathcal{Q} and \mathcal{P} in pp elastic and pp inclusive scattering and showed that, for inclusive scattering, $|\mathcal{Q}|$ and $|\mathcal{P}|$ could each be as large as 10^{-3} - 10^{-4} at currently available energies and transverse momenta. Qualitatively similar results were later obtained by Missimer, Wolfenstein, and Gunion.¹⁷ Parity-violating effects of the same magnitude were also found by Frankfurt and Kopeliovich¹² for two-body and quasi-two-body scattering.

As \sqrt{s} or p_{\perp} increases beyond the ranges considered in Refs. 8-15 and 17 the weak contribution to inclusive differential cross sections may become increasingly important. Eventually the weak interaction should dominate, as can be seen from simple dimensional arguments.¹⁰ Discussions of weak effects in this regime have been given by Craig,¹⁶ and by Halzen.¹⁸

Since pv effects as large as 10^{-3} - 10^{-4} can be expected at currently available energies, and since effects of this size could possibly be detected using existing techniques, the estimates of Refs. 8 and 9 suggest that we examine weak effects at high p_{\perp} in greater detail in an effort to ascertain what can be learned from them. In terms of the previously discussed parton picture of hadron-hadron scattering, pv effects at high p_{\perp} arise from the interference between the strong and weak parton-parton scattering amplitudes. We emphasize that even though the parton-model cross sections result from an *incoherent* sum of the contributions from individual parton-parton scattering processes, the contribution from any *single* scattering is obtained by *coherently* adding the appropriate weak and strong amplitudes. The potential for detecting strong-weak interference effects at the parton level opens up a number of new possibilities for probing the parton model which we will explore in this paper.

The purpose of the present paper is to examine in detail the question of how weak effects at high p_{\perp} can be used to study the parton model, as well as the strong and weak interactions themselves. We will begin in Sec. II by reviewing parton models of inclusive high-energy scattering. Exclusive processes, such as elastic pp scattering, will not be considered further, since the estimates of Ref. 8 indicate that inclusive processes

offer the best hope of measuring \mathcal{G} and \mathcal{P} . Models of the weak parton-parton interaction are considered in Sec. III. Since the detailed form of the neutral-current coupling is not known, several representative possibilities are considered. In addition, a discussion is given of questions relating to the relative phase of the weak and strong parton-parton amplitudes. Computational details are given in Sec. IV and our results are presented and analyzed in Sec. V. Some experimental details are discussed in Sec. VI and our conclusions are given in Sec. VII.

II. STRONG-INTERACTION MODELS

The basis for the present calculations of weak effects at high p_{\perp} is the hard-scattering model of Berman, Bjorken, and Kogut¹⁹ (BBK) shown in Fig. 1 and described in more detail in the Appendix. In this model the initial hadrons a and b are viewed as fragmenting into partons i and j which then undergo a hard scattering. The resulting parton k then decays to produce the hadron c . The parton-parton amplitude, shown in the boxed region of Fig. 1, must be appropriately symmetrized, as indicated in Fig. 2, to account for the possibility that either of the initial partons can scatter to produce the final hadron c .

For purposes of the present calculations a model of strong inclusive high- p_{\perp} scattering called the effective-gluon (EG) model has been developed.^{9,20,21} The EG model is based on an earlier model of the BBK type developed by Ellis and Klinger²² (EK) in which the partons i and j are spin- $\frac{1}{2}$ quarks which scatter via the exchange of a massless, colorless, isoscalar vector gluon. (We shall henceforth identify the partons as quarks and hence use the terms parton and quark somewhat interchangeably.) The EK model has no dimensional parameters (either masses or coupling constants), and hence on naive dimensional grounds the in-

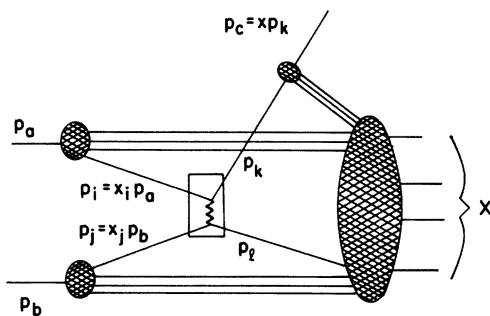


FIG. 1. Parton-model diagram for the process $p(p_a) + p(p_b) \rightarrow c(p_c) + X$. The boxed portion represents the parton-parton scattering process. i , j , k , and l denote partons.

variant cross section at 90° in the c.m. must have the form given by Eq. (1.4) with $n=4$. It is known that $n=4$ is definitely not what is seen experimentally, with $n=6-12$ being more characteristic of the data. The EG model accounts for the observed p_{\perp} dependence (as well as the other features of the single-particle inclusive data for $pp \rightarrow cX$, $c = \pi^\pm, \pi^0, K^\pm, p, \bar{p}$) by multiplying the naive quark-quark-gluon vertex by the function

$$F(\hat{t}) = (1 - \hat{t}/B)^{-1}, \quad B = 18 \text{ (GeV}/c)^2 \quad (2.1)$$

where $-\hat{t}$ is the square of the gluon four-momentum. A detailed discussion of the EG model and an analysis of the experimental data is given in Refs. 20 and 21. For present purposes it is sufficient to note that the EG model accounts for the observed strong-interaction data to within $\sim 10-20\%$ per data point on the average over many orders of magnitude in $Ed\sigma/d^3p$. Since this agreement is usually well within the experimental errors inherent in the data, the EG model is more than adequate for our present purposes.

Although we will use the EG model almost exclusively in what follows below, we mention here two other models that are of interest. The failure of the naive scaling prediction $n=4$ has led to the formulation of the constituent-interchange model^{23,24} (CIM) in which the single hard parton-parton scattering mechanism is replaced by one in which quark-hadron scattering plays a dominant role. In the CIM the observed p_{\perp} dependence is achieved in part by allowing different subprocesses to contribute to the production of mesons and baryons, and to the production of the same observed particles in different kinematic regions. We will return to the CIM in Sec. V, where a comparison will be given of the results for \mathcal{G} using both the EG and the CIM models. The CIM predictions are based on the results of Ref. 17. An interesting result that emerges from this comparison is that a know-

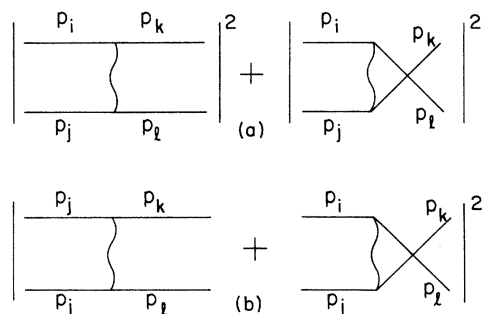


FIG. 2. Cross section for scattering either incident particle into momentum p_k for the case of (a) nonidentical particles and (b) identical particles.

ledge of the functional form of the *weak* parameters $\mathcal{G}(x_1, s)$ and $\mathcal{O}(x_1, s)$ can be used to discriminate between the *strong* EG and CIM models.

More recently a hard parton-parton scattering model similar to the EG model has been introduced by Field and Feynman.²⁵ Their model differs from the EG model primarily in the form of the quark-quark differential cross section, which they take to have the phenomenological form

$$d\hat{\sigma}/d\hat{t} = 2.3 \times 10^6 / (-\hat{s}\hat{t}^3) \mu b \text{ GeV}^6, \quad (2.2)$$

where $\hat{s} = -(p_i + p_j)^2$ and $\hat{t} = -(p_i - p_k)^2$. Since this model is similar to the EG model both in its formulation and in its results, we have confined our calculations to the EG model in the present paper. A comparison of the EG and Field-Feynman models has been given elsewhere,²¹ and a brief discussion of some of the outstanding problems with these models is given in the Appendix.

III. WEAK-INTERACTION MODELS

In the type of parton model discussed in the preceding section there are three broad areas that can be explored through a study of weak effects: the parton distribution functions, the strong parton-parton interaction, and the weak parton-parton interaction. The second area has been discussed in Sec. II,²⁶ and so we turn our attention in this section to the weak interactions. In order to illustrate the sensitivity of the expected weak effects to the assumed form of the hadronic weak interaction we shall calculate \mathcal{G} and \mathcal{O} for several representative weak-interaction models. Before describing the particular models that we have used, we give a brief survey of our present knowledge of the weak Hamiltonian H_w .

Data for both exclusive and inclusive charged-current (CC) interactions are consistent with the following form of the semileptonic charged-current Hamiltonian:

$$H_w^{\text{CC}}(\text{semileptonic}) = \frac{G}{\sqrt{2}} l_\lambda [\cos\theta_C i\bar{u}\gamma_\lambda(1+\gamma_5)d + \sin\theta_C i\bar{u}\gamma_\lambda(1+\gamma_5)s] + \text{H.c.} \quad (3.1)$$

Here, u, d, s represent the field operators for the corresponding quarks, $\theta_C \cong 0.2$ is the Cabibbo angle,²⁷ $G = (1.0262 \pm 0.0001) \times 10^{-5}/m_p^2$ is the Fermi constant,²⁸ and l_λ is the leptonic current,

$$l_\lambda = i\bar{e}\gamma_\lambda(1+\gamma_5)\nu_e + i\bar{\mu}\gamma_\lambda(1+\gamma_5)\nu_\mu. \quad (3.2)$$

In the spirit of the quark model we assume that the nonleptonic (NL) charged-current interaction among quarks is given, in analogy to Eq. (3.1),

by

$$H_w^{\text{CC}}(\text{nonleptonic}) = \frac{G}{\sqrt{2}} [\bar{u}\gamma_\lambda(1+\gamma_5)d] [\bar{d}\gamma_\lambda(1+\gamma_5)u], \quad (3.3)$$

where we have set $\theta_C \cong 0$, an approximation we will use throughout this paper.

The picture with respect to neutral currents is, by contrast, far less clear at the present time. We begin by noting that an unambiguous picture of the space-time structure of the neutral current is still lacking. Hence, although most popular models assume a V, A structure, the possibility that the neutral weak current is actually a combination of S, P , and T has not yet been experimentally ruled out.²⁹ If the current is indeed V, A the relative admixture of V and A is still not certain³⁰ and the same holds true for the relative contributions of different isospin components. In addition to the above uncertainties, there is the added question of whether other quark species exist, in addition to the u, d, s that we have assumed, as suggested by the so-called "high- y anomaly."³¹ Finally the relative strength of the neutral-current and charged-current contributions to the nonleptonic weak Hamiltonian is unknown. In principle this question can be explored by a study of nonleptonic hyperon decays and parity violation in nuclei,³² but few firm conclusions can be drawn at present.

In light of the foregoing discussion it is not surprising that a unique model of the parton-parton weak interaction has not yet emerged from among the many that have been proposed. We will therefore calculate \mathcal{G} and \mathcal{O} for three representative models in order to illustrate the basic features of the calculations and the characteristic results that are obtained. We emphasize that these models have been selected for illustrative purposes only, and not because of their ability to account for existing experimental data.

As our first model we adopt the phenomenological model of Adler and Tuan³³ (AT) in which it is assumed that the neutral current (NC) is an isovector and has the same $V-A$ structure as the charged current. The relative strength of the neutral- and charged-current contributions to H_w is then determined by comparison to experiment. The relative phases of the weak amplitudes for different quark-quark scatterings are not fixed by this phenomenological model, and cannot be determined from νp scattering data which are not sensitive to these phases. We consequently consider two different choices for these phases, and we present below the resulting differences in the expected weak effects. One choice follows from

assigning u , d_θ , s_θ , and c to the weak isospin doublets

$$\begin{pmatrix} u \\ d_\theta \end{pmatrix} \text{ and } \begin{pmatrix} c \\ s_\theta \end{pmatrix}. \quad (3.4)$$

Here c is a charmed quark which is introduced³⁴ to ensure the absence of $\Delta S=1$ neutral currents in the quark model. d_θ and s_θ are the Cabibbo rotated fields, $d_\theta = d \cos\theta_C + s \sin\theta_C$, $s_\theta = s \cos\theta_C - d \sin\theta_C$ which, in the limit $\theta_C=0$, reduce to $d_\theta=d$ and $s_\theta=s$. Since u and c each have $I_3 = +\frac{1}{2}$ while d_θ and s_θ have $I_3 = -\frac{1}{2}$, the total contribution from these quarks to the AT neutral current, which transforms as I_3 , is

$$J_\lambda^{\text{NC}} = \frac{1}{2} [\bar{u}\gamma_\lambda(1+\gamma_5)u - \bar{d}\gamma_\lambda(1+\gamma_5)d + \bar{c}\gamma_\lambda(1+\gamma_5)c - \bar{s}\gamma_\lambda(1+\gamma_5)s]. \quad (3.5)$$

For the processes which we will discuss, all of which involve the production of hadrons which do not contain a valence c quark, c scattering does not contribute and hence will not be considered further. In the approximation of neglecting c the charged current is given by

$$J_\lambda^{\text{CC}} = \bar{u}\gamma_\lambda(1+\gamma_5)d. \quad (3.6)$$

Combining Eqs. (3.5) and (3.6) we can write the effective AT nonleptonic Hamiltonian as

$$H_w^{\text{NL}} = \frac{G}{\sqrt{2}} [(J_\lambda^{\text{CC}})^\dagger J_\lambda^{\text{CC}} + \epsilon (J_\lambda^{\text{NC}})^\dagger J_\lambda^{\text{NC}}] + \text{H.c.}, \quad (3.7)$$

where we have introduced the (real) parameter ϵ to fix the relative strength of the NC and CC contributions to H_w^{NL} . In actually using Eq. (3.7) we have included in both the NC and CC contributions the effect of a W -boson propagator with $m_w = 37$ GeV. Including a finite W -boson mass has the effect of suppressing the large x_1 weak effects compared to what would result from $m_w \rightarrow \infty$. From an analysis of νp data Adler and Tuan have found that $\epsilon = \pm 0.62$.

Equation (3.7) leads to another model of the NL quark-quark interaction if we arbitrarily assume that all the NC quark contributions enter with the same phase. In this case Eq. (3.5) is replaced by

$$J_\lambda^{\text{NC}} = \frac{1}{2} [\bar{u}\gamma_\lambda(1+\gamma_5)u + \bar{d}\gamma_\lambda(1+\gamma_5)d + \bar{c}\gamma_\lambda(1+\gamma_5)c + \bar{s}\gamma_\lambda(1+\gamma_5)s], \quad (3.8)$$

with the understanding that, as before, c makes no contribution. This model is interesting because, by choosing $\epsilon < 0$ in Eq. (3.7), the νp effects arising from different quark-quark scatterings, when calculated using the EG model, will all have the same sign. Since the observed values of G and \mathcal{O} are obtained in the parton model by simply adding the νp effects from the individual quark-quark scatterings, this choice of phases leads to the maximal

effects that can be expected in a model of this type. We shall refer to the two models of Eqs. (3.5) and (3.8) as AT^- and AT^+ , respectively.

A third model of the weak interaction which we shall consider is that developed by Bouchiat, Iliopoulos, and Meyer (BIM),³⁵ which is based on an extension of the Weinberg-Salam³⁶ model to the hadronic sector. The electromagnetic and weak currents are given in this model by

$$J_\lambda^{\text{em}} = \frac{2}{3}\bar{u}\gamma_\lambda u - \frac{1}{3}\bar{d}\gamma_\lambda d - \frac{1}{3}\bar{s}\gamma_\lambda s, \quad (3.9a)$$

$$J_\lambda^{\text{CC}} = \frac{1}{2\sqrt{2}} \frac{1}{\sin\theta_w} \bar{u}\gamma_\lambda(1+\gamma_5)d, \quad (3.9b)$$

$$J_\lambda^{\text{NC}} = \frac{1}{2 \sin^2\theta_w} [\bar{u}\gamma_\lambda(1+\gamma_5)u - \bar{d}\gamma_\lambda(1+\gamma_5)d - \bar{s}\gamma_\lambda(1+\gamma_5)s - 4 \sin^2\theta_w J_\lambda^{\text{em}}], \quad (3.9c)$$

where we have again dropped the c contribution and have set $\theta_C=0$. θ_w is the Weinberg angle whose value is³⁷ $0.3 \leq x_w = \sin^2\theta_w \leq 0.4$. We note that the phases of the various contributions in Eq. (3.9) are determined by the $\text{SU}(2) \otimes \text{U}(1)$ gauge group which is assumed for the interaction. In writing Eq. (3.9) we have ignored the question of quark color. If the quarks are colored, and exchange particles which are color singlets, then the effect of introducing color via the standard three-color model is to reduce the interference term corresponding to identical quark scattering by a factor of $\frac{1}{3}$ relative to the terms arising from \hat{t} - and \hat{u} -channel exchange. The same modification would, of course, occur in the EG model if color were added to it. This complication is not expected to introduce any significant changes into the calculated results and hence we will not include it. However, if the weak interaction were capable of changing color while the strong interaction were not, then the calculated results could change significantly.

In the BIM model the weak Hamiltonian is given by

$$H_w = e(J_\lambda^{\text{CC}} W_\lambda + J_\lambda^{\text{NC}} Z_\lambda) + \text{H.c.}, \quad (3.10)$$

where the currents are those defined in Eq. (3.9), and e is the electric charge. W_λ and Z_λ are the field operators for the charged and neutral vector bosons respectively whose masses (in GeV) are fixed by the theory to be

$$m_w = 37.3/\sin\theta_w, \quad m_z = 74.6/\sin 2\theta_w. \quad (3.11)$$

The Fermi constant is given by

$$\frac{G}{\sqrt{2}} = \frac{1}{m_w^2} \left(\frac{e}{2\sqrt{2} \sin\theta_w} \right)^2. \quad (3.12)$$

Since virtually all models of H_w^{NL} incorporate the

charged-current contribution given in Eq. (3.3), we will also present results for a model in which Eq. (3.3) gives the entire contribution to H_w^{NL} . By comparing the predictions of this model, which is essentially the naive Cabibbo model, to those of other models we can learn what effect the inclusion of various neutral-current contributions has on the expected size of \mathcal{G} and \mathcal{P} .

Having specified the phases of the various contributions to the nonleptonic weak Hamiltonian H_w^{NL} , there remains the question of the relative phases of the weak and strong quark-quark scattering amplitudes. It is important in a discussion of phases to bear in mind that the magnitude and sign of both \mathcal{G} and \mathcal{P} are actually determined by an intricate combination of *two* different kinds of phase effects. In the first place \mathcal{G} and \mathcal{P} for any individual quark-quark scattering process are determined by the *coherent* interference of the weak and strong amplitudes, which depends on the relative phase between the weak model and the EG model contributions. Secondly the calculated values of \mathcal{G} and \mathcal{P} for the observed hadrons depends on an *incoherent* sum of the individual quark-quark scattering contributions. Hence it is possible to have large effects at the quark-quark level and nonetheless have \mathcal{G} and \mathcal{P} small due to cancellations among the contributions from the individual quark-quark scatterings. We will later show in fact that for a range of values of $\sin\theta_w$ in the BIM model, $\mathcal{G} \approx \mathcal{P} \approx 0$ even

though the individual contributions are relatively large.

It is important to emphasize that, in the parton model where different qq scatterings are added incoherently, simple cross-section measurements are not sensitive to either of the phases discussed above. Hence, in developing the EG model of strong qq scattering the question of strong-interaction phases has not been addressed. The question of phases can be resolved only by measuring interference phenomena such as those discussed here.

To fix the relative weak-strong phase, an assumption must be made concerning the origin of the EG amplitude in Ref. 20. If this amplitude results from some complicated mechanism such as multi-gluon exchange, then the strong phases will depend on the precise details of the interaction and cannot be determined *a priori*. On the other hand, we can interpret the EG amplitude as a strong-interaction form-factor modification of the one-gluon-exchange amplitude, where the gluon couples to the baryon number of the quarks. This determines the phase of the EG amplitude relative to the weak amplitude, provided we assume that the weak interactions are also mediated by vector fields. In this case (which we will assume in the calculations below) the interference between the weak and strong amplitudes will be maximally constructive.

IV. ASYMMETRY AND POLARIZATION CALCULATIONS

Having discussed the input which is needed to calculate pv effects at large p_1 , we turn now to a description of the details of the calculations. To calculate the asymmetry \mathcal{G} defined in Eq. (1.5), it is necessary to determine the inclusive cross section, $pp \rightarrow cX$, for the case where one of the incident protons is polarized with \pm helicity. For a positive helicity proton incident on an unpolarized proton we have

$$E \frac{d\sigma^+}{d^3p} = \frac{1}{\pi s} \sum_{ij} \int \frac{dx dx_i}{x^2 (xx_i - x_1)} \left\{ u_i^{++}(x_i) u_j \left(\frac{x_i x_2}{xx_i - x_1} \right) [f_{ij}^+(x_1, x_2, s; x_i, x) G_{i/c}(x) + f_{ij}^{\prime+}(x_1, x_2, s; x_i, x) G_{j/c}(x) + \delta_{ij} f_{ij}^{\prime\prime+}(x_1, x_2, s; x_i, x) G_{i/c}(x)] \right. \\ \left. + u_i^{+-}(x_i) u_j \left(\frac{x_i x_2}{xx_i - x_1} \right) [f_{ij}^-(x_1, x_2, s; x_i, x) G_{i/c}(x) + f_{ij}^{\prime-}(x_1, x_2, s; x_i, x) G_{j/c}(x) + \delta_{ij} f_{ij}^{\prime\prime-}(x_1, x_2, s; x_i, x) G_{i/c}(x)] \right\}. \quad (4.1)$$

In Eq. (4.1) $u_i^{+(\pm)}$ are the number of quarks of type i with (\pm) helicity in a proton of helicity $+$. $f^{\pm}, f^{\prime\pm}, f^{\prime\prime\pm}$ describe the dynamics of the scattering of a quark with \pm helicity from an unpolarized quark, and, in analogy with the definitions of the Appendix,

$$d\hat{\sigma}_{ij}^{\pm} = f_{ij}^{\pm}(x_1, x_2, s; x_i, x) d\hat{x}_i, \text{ etc.} \quad (4.2)$$

The polarized distribution functions are discussed in Ref. 38 whose notation we follow. An equation for $E d\sigma^-/d^3p$ can be obtained by making the replacement $u_i^{+(\pm)} \rightarrow u_i^{-(\pm)}$. Using the symmetry³⁸ $u^{++} = u^{--}$ and $u^{+-} = u^{-+}$ we subtract the \pm helicity cross sections to get

$$E \frac{d\sigma^+}{d^3p} - E \frac{d\sigma^-}{d^3p} = \frac{1}{\pi s} \sum_{ij} \int \frac{dx_i dx_j}{x^2(xx_i - x_j)} \left\{ [u_i^{++}(x_i) - u_i^{+-}(x_i)] \mu_j \left(\frac{x_i x_j}{xx_i - x_j} \right) \right. \\ \left. \times [(f_{ij}^+ - f_{ij}^-) G_{i/c} + (f_{ij}^{'+} - f_{ij}^{\prime-}) G_{j/c} + \delta_{ij} (f_{ij}^{\prime\prime+} - f_{ij}^{\prime\prime-}) G_{i/c}] \right\}. \quad (4.3)$$

To evaluate the sum over i we assume that only the valence quarks are polarized. Using the notation and results of Ref. 38,

$$E \frac{d\sigma^+}{d^3p} - E \frac{d\sigma^-}{d^3p} = \frac{1}{\pi s} \sum_j \int \frac{dx_i dx_j}{x^2(xx_i - x_j)} \{ (2\alpha - 1) u_v \mu_j [(f_{uj}^+ - f_{uj}^-) G_{u/c} + (f_{uj}^{\prime+} - f_{uj}^{\prime-}) G_{j/c} + \delta_{uj} (f_{uj}^{\prime\prime+} - f_{uj}^{\prime\prime-}) G_{u/c}] \\ + (2\beta - 1) d_v \mu_j [(f_{dj}^+ - f_{dj}^-) G_{d/c} + (f_{dj}^{\prime+} - f_{dj}^{\prime-}) G_{j/c} + \delta_{dj} (f_{dj}^{\prime\prime+} - f_{dj}^{\prime\prime-}) G_{d/c}] \}, \quad (4.4)$$

where the values of α and β depend upon the model of the polarized distribution functions.³⁸ u_v (d_v) denotes the u (d) valence contribution.

Over the range of s and p_\perp which are experimentally accessible we expect the weak amplitude to be much smaller than the strong amplitude for any scattering process. Consequently the denominator of Eq. (1.5) can be taken to be equal to twice the strong inclusive cross section $E d\sigma_s/d^3p$. We shall concentrate on calculations based on the EG model which is known to reproduce the experimental strong cross sections, and use the polarized distribution functions developed in Ref. 38 which provide an adequate description of the polarized electron-proton scattering data. Therefore in order to calculate the weak asymmetries expected in inclusive π^+ production we need only calculate the expressions for $f_{ij}^+ - f_{ij}^-$, etc., which result from different weak models.

In the EG model the number of terms in Eq. (4.4)

is reduced further by the assumption that the scattered quark appears as a valence quark of the observed particle. Thus for π^+ production we consider only those contributions where a u or a \bar{d} quark is scattered into momentum p_k , as shown in Fig. 1. The terms that will appear in Eq. (4.4) are

$$(f_{uj}^+ - f_{uj}^-), \quad j = u, d, s, \bar{u}, \bar{d}, \bar{s}, \\ (f_{uj}^{\prime+} - f_{uj}^{\prime-}), \quad j = u, \bar{d}, \\ (f_{uu}^{\prime\prime+} - f_{uu}^{\prime\prime-}), \\ (f_{dj}^{\prime+} - f_{dj}^{\prime-}), \quad j = u, \bar{d}. \quad (4.5)$$

As an example of these calculations we consider, in the BIM weak model, the quantity $f_{ud}^+ - f_{ud}^-$ which results when a u quark from proton a of Fig. 1 is polarized with \pm helicity and scatters into momentum p_k from a d quark of proton b . If ω is the polarization vector of the u quark (with momentum p_i), then the transition matrix element may be written as

$$\mathfrak{M} = \frac{4\pi\alpha_s}{q^2} F^2(q^2) \bar{u}(p_k) \gamma_\mu u_\omega(p_i) \bar{d}(p_l) \gamma_\nu d(p_j) \\ + \left(\frac{e}{2\sqrt{2} \sin\theta_w} \right)^2 \left(\frac{\delta_{\mu\nu} + q'_\mu q'_\nu / m_w^2}{q'^2 + m_w^2} \right) \bar{u}(p_k) \gamma_\mu (1 + \gamma_5) d(p_j) \bar{d}(p_l) \gamma_\nu (1 + \gamma_5) u_\omega(p_i) \\ - \left(\frac{e}{2 \sin 2\theta_w} \right)^2 \left(\frac{\delta_{\mu\nu} + q_\mu q_\nu / m_z^2}{q^2 + m_z^2} \right) \bar{u}(p_k) \gamma_\mu (a + \gamma_5) u_\omega(p_i) \bar{d}(p_l) \gamma_\nu (b + \gamma_5) d(p_j), \quad (4.6)$$

where $q^2 = (p_k - p_i)^2$ and $q'^2 = (p_l - p_i)^2$. The first term is the EG model amplitude of Sec. II and Ref. 20. The second and third terms correspond to the charged- and neutral-current amplitudes of the BIM model, and we have used the notation

$$a = (1 - \frac{8}{3} x_w), \\ b = (1 - \frac{4}{3} x_w), \quad (4.7)$$

for the quantities which result from the neutral-current expression of Eq. (3.9c). The Dirac equation, coupled with the assumption that the mass of the quarks can be neglected, can be used to eliminate the terms proportional to $q_\mu q_\nu$ and $q'_\mu q'_\nu$ in Eq. (4.6). The square of the matrix element may

be written as

$$\sum_{\text{spins}} |\mathfrak{M}|^2 = \sum_{\text{spins}} (|\mathfrak{M}_s|^2 + |\mathfrak{M}_w|^2 + 2 \text{Re} \mathfrak{M}_s \mathfrak{M}_w^*), \quad (4.8)$$

where the first term is just the square of the strong-interaction matrix element, the second term is the square of the weak-interaction matrix element, and the third term is the interference between the strong and weak amplitudes. We note that since the strong interaction is parity conserving it will be independent of the longitudinal polarization of the u quark and hence will not contribute to the quantity $f^+ - f^-$. The weak interaction will

contribute a term to $f^+ - f^-$, since the weak interaction is parity violating, but the contribution will be of order G^2 , compared to the weak-strong interference contribution which will be of order $G\alpha_s$. Hence we may safely neglect the purely weak asymmetry with respect to the weak-strong asymmetry. Using this, and the relation

$$\begin{aligned} d\hat{\sigma}^\pm &= \frac{1}{16\pi\hat{s}} \sum_{\text{spins}} |\mathfrak{M}(\omega = \pm p_i)|^2 d\hat{x}_1 \\ &= f^\pm d\hat{x}_1, \end{aligned} \quad (4.9)$$

we may write

$$\begin{aligned} f_{ud}^+ - f_{ud}^- &= \frac{1}{8\pi\hat{s}} \text{Re} \sum_{\text{spins}} [\mathfrak{M}_s \mathfrak{M}_w^*(\omega = +p_i) \\ &\quad - \mathfrak{M}_s \mathfrak{M}_w^*(\omega = -p_i)]. \end{aligned} \quad (4.10)$$

The matrix element of Eq. (4.6) may be used to evaluate the expressions in Eq. (4.10), with the re-

$$\begin{aligned} (f_{uu}^+ + f_{uu}^{\prime+} + f_{uu}^{\prime\prime+}) - (f_{uu}^- + f_{uu}^{\prime-} + f_{uu}^{\prime\prime-}) &= \frac{2\alpha_s G s a}{\sqrt{2}} \left[\frac{F^2(\hat{t})}{\hat{t}(1-\hat{t}/m_z^2)} + \frac{F^2(\hat{t})}{\hat{t}(1-\hat{u}/m_z^2)} + \frac{F^2(\hat{u})}{\hat{u}(1-\hat{u}/m_z^2)} + \frac{F^2(\hat{u})}{\hat{u}(1-\hat{t}/m_z^2)} \right], \\ f_{us}^+ - f_{us}^- &= -\frac{\alpha_s G}{\sqrt{2}\hat{s}} \frac{F^2(\hat{t})}{\hat{t}(1-\hat{t}/m_z^2)} [(a+b)\hat{s}^2 - (a-b)\hat{u}^2], \\ f_{u\bar{u}}^+ - f_{u\bar{u}}^- &= -\frac{2\alpha_s G}{\sqrt{2}\hat{s}} \frac{F^2(\hat{t})}{\hat{t}(1-\hat{t}/m_z^2)} a\hat{u}^2, \\ f_{u\bar{d}}^+ - f_{u\bar{d}}^- &= f_{us}^+ - f_{us}^- = \frac{\alpha_s G}{\sqrt{2}\hat{s}} \frac{F^2(\hat{t})}{\hat{t}(1-\hat{t}/m_z^2)} [(a+b)\hat{u}^2 - (a-b)\hat{s}^2], \\ f_{u\bar{d}}^{\prime+} - f_{u\bar{d}}^{\prime-} &= \frac{\alpha_s G}{\sqrt{2}\hat{s}} \frac{F^2(\hat{u})}{\hat{u}(1-\hat{u}/m_z^2)} [(a+b)\hat{t}^2 - (a-b)\hat{s}^2], \\ f_{d\bar{u}}^{\prime+} - f_{d\bar{u}}^{\prime-} &= -\frac{2\alpha_s G}{\sqrt{2}\hat{s}} \left\{ 2\hat{s}^2 \frac{F^2(\hat{u})}{\hat{u}(1-\hat{t}/m_z^2)} + \frac{1}{2} \frac{F^2(\hat{u})}{\hat{u}(1-\hat{u}/m_z^2)} [(a+b)\hat{s}^2 + (a-b)\hat{t}^2] \right\}, \\ f_{d\bar{d}}^{\prime+} - f_{d\bar{d}}^{\prime-} &= -\frac{2\alpha_s G}{\sqrt{2}\hat{s}} b\hat{t}^2 \frac{F^2(\hat{u})}{\hat{u}(1-\hat{u}/m_z^2)}. \end{aligned} \quad (4.13)$$

Contributions from annihilation processes, such as $u\bar{u} \rightarrow Z^0 \rightarrow u\bar{u}$, have not been included since these are highly suppressed for kinematic reasons. A discussion of this point is given in footnote 16 of Ref. 20. The expressions in Eqs. (4.13) may be substituted into Eqs. (4.4) and (1.5), along with specific values α and β from Ref. 38 which describe the polarized distribution functions, to evaluate the π^+ asymmetry.

To evaluate the quantities $f^+ - f^-$ in the Adler-Tuan model we need only let $a = b = \epsilon = 0.62$ in the expressions of Eq. (4.13). This simple substitution will be true *only* for the evaluation of $f^+ - f^-$, and is not true for relating cross sections in the two models. The simple substitution is a result of the fact that the asymmetry arising from neutral currents depends linearly on the parity-violating

sult

$$\begin{aligned} f_{ud}^+ - f_{ud}^- &= -\frac{2\alpha_s G}{\sqrt{2}\hat{s}} \left\{ 2\hat{s}^2 \frac{F^2(\hat{t})}{\hat{t}(1-\hat{u}/m_z^2)} \right. \\ &\quad \left. + \frac{1}{2} \frac{F^2(\hat{t})}{\hat{t}(1-\hat{t}/m_z^2)} \right\} \\ &\quad \times [(a+b)\hat{s}^2 - (a-b)\hat{u}^2], \end{aligned} \quad (4.11)$$

where $\hat{t} = -(p_k - p_i)^2$, $\hat{u} = -(p_i - p_j)^2$, $\hat{s} = -(p_i + p_j)^2$, and we have used Eq. (3.12) to write the expression in terms of G . The kinematic relations

$$\begin{aligned} \hat{t} &= -x_2 x_i s / x, \\ \hat{u} &= -x_1 x_2 x_i s / [x(x x_i - x_1)], \\ \hat{s} &= x_2 x_i^2 s / (x x_i - x_1) \end{aligned} \quad (4.12)$$

can be used to express Eq. (4.11) in the form needed to evaluate Eq. (4.4). The remaining terms needed to evaluate Eq. (4.4) are

lating product of the V and A portions of the weak interaction. In the case of the BIM model, the neutral weak coupling can be expressed schematically in the form

$$\begin{aligned} H_w^{NC} &\sim (aV_1 + A_1)(bV_2 + A_2) \\ &= abV_1V_2 + (aV_1A_2 + bA_1V_2) + A_1A_2, \end{aligned} \quad (4.14)$$

where $V_{1,2}$ and $A_{1,2}$ are the vector and axial-vector portions of the two interacting currents. The neutral-current weak interaction in the Adler-Tuan model is of the form

$$\begin{aligned} H_w^{NC} &\sim \epsilon(V_1 + A_1)(V_2 + A_2) \\ &= \epsilon[V_1V_2 + (V_1A_2 + A_1V_2) + A_1A_2]. \end{aligned} \quad (4.15)$$

The asymmetry will result only from the VA and AV terms. Setting $a = b = \epsilon$ reduces the VA term

of Eq. (4.14) to the form of Eq. (4.15) and allows us to easily evaluate the asymmetries in the Adler-Tuan model. To obtain the charged-current results simply set $a=b=\epsilon=0$ in Eqs. (4.13). The correct sign to be used with each term in Eq. (4.13) must be determined individually for the various weak models.

Evaluation of the Λ longitudinal polarization which results from the presence of the weak interaction can be carried out in a similar manner. In

$$E \frac{d\sigma_+}{d^3p} = \frac{1}{\pi s} \sum_{ij} \int \frac{dx dx_i}{x^2(xx_i - x_1)} u_i(x_i) u_j\left(\frac{x_1 x_2}{xx_i - x_1}\right) \times [f_{ij+}(x_1, x_2, s; x_i, x) G_{i/c}(x) + f'_{ij+}(x_1, x_2, s; x_i, x) G_{j/c}(x) + \delta_{ij} f''_{ij+}(x_1, x_2, s; x_i, x) G_{i/c}(x)], \quad (4.16)$$

where $f_{ij+}, f'_{ij+}, f''_{ij+}$ describe the quark scattering cross sections for the production of a quark with momentum p_h (see Fig. 1) and positive helicity. $E d\sigma_+/d^3p$ is obtained by letting $+-$ in Eq. (4.16). Consequently we may write

$$\frac{E d\sigma_+}{d^3p} - \frac{E d\sigma_-}{d^3p} = \frac{1}{\pi s} \sum_{ij} \int \frac{dx dx_i}{x^2(xx_i - x_1)} u_i u_j [(f_{ij+} - f_{ij-}) G_{i/c} + (f'_{ij+} - f'_{ij-}) G_{j/c} + \delta_{ij} (f''_{ij+} - f''_{ij-}) G_{i/c}]. \quad (4.17)$$

Again the weak amplitude will be much smaller than the strong amplitude for experimentally available kinematics, and hence the denominator of Eq. (1.6) can be approximated by $E d\sigma_s/d^3p$, which is easily evaluated in the EG model.

In the EG model the Λ can result from the decay of u , d , and s quarks and thus terms corresponding to the scattering of these quarks must be included in evaluating Eq. (4.17). Again the weak-induced longitudinal polarization will result principally from the interference of the strong amplitude with the pv portion of the weak amplitude, and the parity violation which arises solely from the square of the weak amplitude can be neglected. The quantities $f_+ - f_-$ can be evaluated in a way completely analogous to the π^+ case, where now ω represents the polarization vector of the quark in the final state with momentum p_h . In the case of both π^+ and Λ production the observed pv effects are the result of parity violation in the quark-quark scattering, and thus we expect the two cases to yield results of comparable magnitude. That this is indeed the case is shown in the next section.

For the EG model the numerator of Eqs. (1.5) and (1.6) for \mathcal{Q} and \mathcal{P} will each be proportional to $\alpha_s \kappa_c$, where $\alpha_s = g_s^2/4\pi$, g_s is the strong-interaction quark-quark-gluon coupling constant, and κ_c is the constant associated with the quark decay function $G_{i/c}$ defined in Ref. 20. The denominator of these expressions is just the strong-interaction cross section and hence, in the EG model, is proportional to the constant $\alpha_s^2 \kappa_c$. Consequently \mathcal{Q}

and \mathcal{P} will be independent of the value of κ_c and inversely proportional to α_s . The value of α_s was extracted from the fits of the EG model,²⁰ and we will use the value $\alpha_s = 3.0$ in evaluating \mathcal{Q} and \mathcal{P} .

V. RESULTS FOR \mathcal{Q} AND \mathcal{P}

The enhancement of weak effects at large transverse momentum which occurred in the rough calculations of Ref. 8 appears in our more detailed calculations as a general feature of the models we consider. As is emphasized below, however, there are models in which the weak effects can actually pass through zero and change sign for a nonzero value of x_\perp , although in these cases a rapid increase in \mathcal{Q} or \mathcal{P} is predicted for values of x_\perp greater than the value at which the zero occurs.

Our results show that in models of inclusive scattering based on a quark-quark scattering mechanism, the size of expected weak pv effects generally increases by a factor of $\sim 10^3$ over a range of x_\perp from $x_\perp = 0.1$ to $x_\perp = 0.6$, and that a similar increase is observed at fixed x_\perp for a range of center-of-momentum energy \sqrt{s} from $\sqrt{s} = 20$ GeV to $\sqrt{s} = 65$ GeV. Although all models based on the hard scattering of proton constituents predict an increase of weak-interaction effects with increasing x_\perp , the detailed dependence of \mathcal{Q} and \mathcal{P} on the kinematic variables, and the exact magnitude of the expected effects, differ with the form assumed for the strong and weak interactions. The size of the effects can also depend upon the as-

sumed form of the quark distribution functions. Thus measurements of pv effects may be able to distinguish among various proposed models of the interactions and distributions.

We first consider the asymmetry \mathcal{G} expected in the process $pp \rightarrow \pi^+ X$. As discussed in Sec. VI below, π^+ production is expected to have the smallest background contamination, which is the reason we have focused on this channel. The results of using different forms of the polarized distribution functions are shown in Fig. 3. The curves of Fig. 3 are based on the EG model of the strong interaction and the previously discussed AT^+ model of the weak interaction. We have assumed, as we shall throughout our discussion, that the weak and strong amplitudes for each quark-quark scattering process combine to provide a maximal quark-quark interference effect. As the figure indicates, the result of using the different distribution functions of Ref. 38 is simply to change the overall size of the expected effects and does not change the dependence of \mathcal{G} on the variables x_1 and s . The asymmetries obtained using the SU(6) form of the polarized distribution functions³⁹ are a factor of 1.3 larger than the results using the dis-

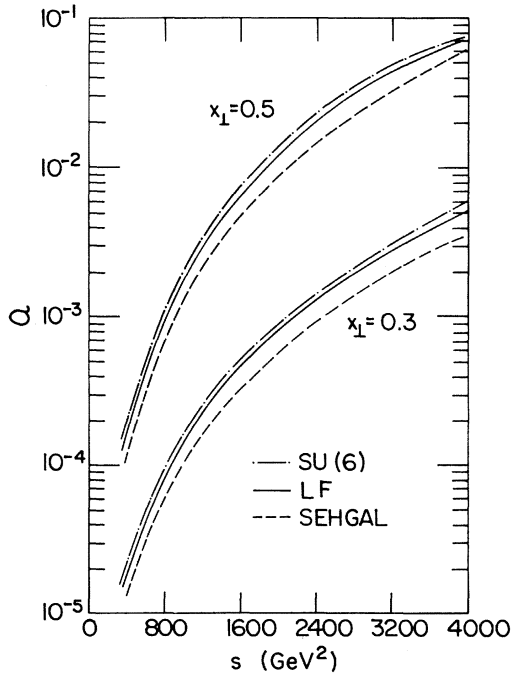


FIG. 3. Variation in $\mathcal{G}(\pi^+)$ at $\theta_{c.m.} = 90^\circ$ which results from assuming different forms for the quark distribution functions in a polarized proton. The calculations are based on the EG model of the strong interaction and the AT^+ model of the weak interaction. The polarized distribution functions are derived in Ref. 38.

tributions of Sehgal,⁴⁰ and those distributions which we derived elsewhere³⁸ (labeled LF in the figure) lie between these two cases. The differences result from the fact that different models of the polarized distributions lead to different values of α and β in Eq. (4.4) and thus weight the quark-quark scattering processes by different relative amounts. If these different distributions are used in conjunction with other models of the weak interaction similar results are obtained. There may, however, exist combinations of the phases and coefficients of the individual quark-quark scatterings which conspire to produce larger variations in the asymmetries for different distribution models. We shall use the LF form of the distributions for illustrative purposes to demonstrate the expected results. It should be kept in mind, however, that the asymmetries can change if different functions are used.

Tables I and II and Figs. 4 and 5 show the results of assuming different models of the weak and strong interactions in our calculations. The strong inclusive cross section is obtained from the EG model and we use the LF polarized distribution functions. We first present the asymmetries that are expected if only charged-current interactions are present, and then the effect of using different models of the neutral weak currents is displayed by presenting the ratio of the asymmetries expected for these different models to the charged-current predictions. Table I displays the s dependence at fixed x_1 for two intermediate values of x_1 , and Table II displays the x_1 behavior at fixed s . An analysis of the functional dependence of the asymmetry on the variables x_1 and s in the CC model shows that, for fixed values of x_1 , the s dependence can be well represented as a power law of the form s^m , with m ranging from ~ 1.5 for small x_1 to ~ 3.0 for larger x_1 . Similarly at fixed values of s , the x_1 dependence can also be approximated by a power law of the form $x_1^{3.9}$ at $\sqrt{s} = 20$ GeV to $x_1^{4.7}$ for $\sqrt{s} = 63$ GeV. However, the fact that the exponents of x_1 and s are not constant indicates that \mathcal{G} is actually a more complicated function of these two variables. Tables I and II also indicate that models including neutral currents tend, in general, to predict a slightly more rapid increase of \mathcal{G} with x_1 and s than does the charged-current model.

In Fig. 4 we also show the results for \mathcal{G} obtained from the constituent-interchange model.¹⁷ We have arbitrarily adjusted the normalization of the CIM results to agree with the EG model results at $x_1 = 0.3$ and $s = 400$ GeV² in order to demonstrate more clearly the differences in the s and x_1 behaviors found in the two models. The CIM predicts¹⁷ an asymmetry which increases as $\mathcal{G} \propto p_1^2$

TABLE I. Invariant cross sections and calculated values of the asymmetry parameter \mathcal{G} for $pp \rightarrow \pi^* X$ at $\theta_{\text{c.m.}} = 90^\circ$ and $x_1 = 0.3$ and 0.5 . \mathcal{G} is defined in Eq. (1.5), the strong cross sections are calculated using the EG model, and the LF quark distributions of Ref. 38 are used. CC denotes the contribution from the charged currents alone, while AT* and BIM are the neutral-current models discussed in Sec. III. Note that for $x_w = \frac{1}{3}$ in the BIM model \mathcal{G} vanishes for all values of s at some value of x_1 between 0.3 and 0.5 .

s (GeV ²)	$Ed\sigma/d^3p$ (cm ² c ³ GeV ⁻²)	\mathcal{G} (CC)	AT*/CC	AT ⁻ /CC	BIM/CC		
					$x_w = \frac{1}{3}$	$x_w = \frac{3}{8}$	$x_w = \frac{2}{5}$
$x_1 = 0.3$							
400	4.1×10^{-32}	2.9×10^{-6}	6.6	-3.9	0.16	1.2	1.7
800	1.8×10^{-32}	1.3×10^{-5}	6.7	-4.0	0.16	1.2	1.7
1200	2.5×10^{-34}	3.3×10^{-5}	6.8	-4.0	0.16	1.2	1.7
1600	5.6×10^{-35}	6.6×10^{-5}	6.8	-4.1	0.15	1.2	1.7
2000	1.7×10^{-35}	1.2×10^{-4}	7.0	-4.2	0.15	1.2	1.8
2400	6.4×10^{-36}	1.8×10^{-4}	7.1	-4.3	0.15	1.2	1.8
2800	2.7×10^{-36}	2.7×10^{-4}	7.2	-4.3	0.14	1.2	1.8
3200	1.3×10^{-36}	3.9×10^{-4}	7.3	-4.4	0.14	1.2	1.8
3600	6.7×10^{-37}	5.3×10^{-4}	7.4	-4.4	0.14	1.3	1.8
4000	3.7×10^{-37}	6.9×10^{-4}	7.4	-4.5	0.14	1.3	1.9
$x_1 = 0.5$							
400	2.5×10^{-35}	2.1×10^{-5}	7.9	-5.2	-0.07	1.2	1.8
800	6.6×10^{-37}	1.2×10^{-4}	8.3	-5.5	-0.08	1.2	1.9
1200	7.0×10^{-38}	3.4×10^{-4}	8.5	-5.6	-0.09	1.3	2.0
1600	1.4×10^{-38}	7.4×10^{-4}	8.7	-5.7	-0.10	1.3	2.0
2000	3.8×10^{-39}	1.3×10^{-3}	9.0	-5.9	-0.11	1.3	2.1
2400	1.3×10^{-39}	2.2×10^{-3}	9.2	-6.1	-0.12	1.3	2.1
2800	5.4×10^{-40}	3.3×10^{-3}	9.4	-6.2	-0.13	1.4	2.1
3200	2.5×10^{-40}	4.6×10^{-3}	9.8	-6.6	-0.14	1.4	2.2
3600	1.2×10^{-40}	6.5×10^{-3}	9.9	-6.7	-0.15	1.4	2.2
4000	6.7×10^{-41}	8.5×10^{-3}	10.1	-6.8	-0.16	1.4	2.3

$= 4sx_1^2$, which is to be compared with the EG results presented in the last paragraph. The difference in the predictions of the two strong-interaction models for the *same* weak model is clearly shown in Fig. 4, and hence by measuring weak effects at large p_\perp it may be possible to distinguish among models of the strong inclusive processes which are each capable of reproducing the strong data.

Another feature which emerges from the analysis of \mathcal{G} is the strong dependence of the results on the value of x_w in the Weinberg-Salam-type weak model of BIM. The graphs of Fig. 6 demonstrate this variation, and show that for some values of x_w the asymmetry can actually change sign as one increases the value of x_1 . This sensitivity can again be traced to a combination of the choice of phases and to the value of the coefficients which multiply individual quark-quark asymmetry terms in Eq. (4.4). This indicates that these factors can combine to yield a zero value for the π^* asymmetry even though the individual quark-quark scattering amplitudes interfere maximally. The value of x_w [or of a and b in Eq. (4.7)] for which this occurs will, of course, depend upon which polarized

distributions are used—a consequence of the fact that the α and β which characterize the polarized distributions will also affect the weighting of the individual q - q scatterings as seen in Eq. (4.4). Hence, the measurement of pv effects could prove to be a sensitive indicator of any of these parameters should the others become known from some other source. Asymmetries of the same size which we present here for the π^* will also be expected in the inclusive production of other particles.

The results of our calculations for the longitudinal polarization of inclusively produced Λ 's at large p_\perp are presented in Tables III and IV and in Figs. 7 and 8. The Λ polarization at constant x_1 may be parameterized in the form $\mathcal{P} \propto s^{2.5}$ at $x_1 = 0.3$ and $\mathcal{P} \propto s^{2.7}$ for $x_1 = 0.5$. The constant s curves are roughly of the form $\mathcal{P} \propto x_1^{3.6}$ for $\sqrt{s} = 20$ GeV and $\mathcal{P} \propto x_1^{4.5}$ for $\sqrt{s} = 63$ GeV (although this form is true really only for $x_1 \gtrsim 0.2$). This is of the same form as our parameterization of $\mathcal{G}(\pi^*)$, although both the s and x_1 dependences are slightly lower for the Λ polarization. Another fact which can be noted from Tables III and IV is that, except for the AT⁻ model, there is little difference in the shape of the polarization curves obtained by using different weak models.

TABLE II. Invariant cross sections and calculated values of the asymmetry parameter \mathcal{Q} for $pp \rightarrow \pi^+ X$ at $\theta_{\text{c.m.}} = 90^\circ$ and $s = 400, 2200,$ and 4000 GeV^2 . \mathcal{Q} is defined in Eq. (1.5), the strong cross sections are calculated using the EG model, the LF quark distribution functions of Ref. 38 are used, and the weak models are defined in the text. See also caption to Table I.

x_\perp	$E d\sigma/d^3p$ ($\text{cm}^2 c^3 \text{ GeV}^{-2}$)	\mathcal{Q} (CC)	AT ⁺ /CC AT ⁻ /CC		BIM/CC		
					$x_W = \frac{1}{3}$	$x_W = \frac{3}{8}$	$x_W = \frac{2}{5}$
$s = 400 \text{ GeV}^2$							
0.1	4.1×10^{-28}	1.7×10^{-7}	5.3	-2.7	0.37	1.1	1.5
0.2	2.6×10^{-30}	8.3×10^{-7}	5.9	-3.2	0.28	1.1	1.6
0.3	4.2×10^{-32}	2.9×10^{-6}	6.5	-3.9	0.16	1.2	1.7
0.4	9.5×10^{-34}	8.4×10^{-6}	7.3	-4.6	0.05	1.2	1.8
0.5	2.5×10^{-35}	2.0×10^{-5}	7.9	-5.2	-0.07	1.2	1.8
0.6	6.2×10^{-37}	4.1×10^{-5}	9.0	-6.2	-0.60	1.3	2.0
$s = 2200 \text{ GeV}^2$							
0.1	1.8×10^{-30}	1.3×10^{-6}	6.3	-3.3	0.40	1.3	1.8
0.2	2.0×10^{-33}	2.0×10^{-5}	6.7	-3.8	0.29	1.3	1.8
0.3	1.0×10^{-35}	1.4×10^{-4}	7.4	-4.4	0.15	1.3	1.9
0.4	1.2×10^{-37}	6.0×10^{-4}	7.9	-5.0	0.03	1.3	1.9
0.5	2.2×10^{-39}	1.8×10^{-3}	8.6	-5.7	-0.11	1.2	2.0
0.6	4.3×10^{-41}	4.4×10^{-3}	9.3	-6.5	-0.25	1.2	2.0
$s = 4000 \text{ GeV}^2$							
0.1	1.7×10^{-31}	4.4×10^{-6}	5.5	-2.9	0.32	1.1	1.5
0.2	9.7×10^{-35}	8.7×10^{-5}	6.3	-3.6	0.26	1.2	1.7
0.3	3.7×10^{-37}	6.9×10^{-4}	7.4	-4.5	0.14	1.3	1.8
0.4	4.0×10^{-39}	2.9×10^{-3}	8.7	-5.6	0.06	1.3	2.1
0.5	6.7×10^{-41}	8.5×10^{-3}	10	-6.8	-0.16	1.4	2.3
0.6	1.3×10^{-42}	1.6×10^{-2}	14	-9.5	-0.42	1.8	2.9

This suggests that for a wide range of models, the dependence of $\mathcal{P}(\Lambda)$ on s and x_\perp is a characteristic of our quark-quark scattering model and is not particularly sensitive to the details of the weak model. There is, however, an order-of-magnitude difference in the size of the polarization predicted using different weak interactions so that, if the EG model is the correct model of the strong interaction between quarks, then polarization measurements can help to decide among proposed weak models.

The results obtained using the Adler-Tuan model with different choices of phases emphasizes, again, the important role that phases play in the determination of weak effects. As is seen in Table IV, the polarization can change sign as one increases x_\perp at fixed s in the AT⁻ model. As was the case for the BIM model with $x_W = 0.3$ in the calculation of $\mathcal{Q}(\pi^+)$, one is observing the cancellation of weak effects occurring in different quark-quark scatterings.

In the EG model the polarizations given in Tables III and IV should also apply to the process $pp \rightarrow pX$. This results from the similarity of the quark-quark structure for p and Λ production in the EG model. To be more explicit, the major contribu-

tion to both p and Λ production comes from the scattering and subsequent decay of u and d quarks in the EG model. The additional contribution to the Λ cross section which comes from the scattering of s quarks is small compared to the valence u and d scattering contributions. The normalization of the Λ cross sections, as reflected in the EG model constant κ_Λ , is expected to be smaller than the corresponding normalization of the proton cross section,⁴¹ but \mathcal{P} is independent of these normalizations (it depends only on the strong quark scattering constant α_s) and hence the p and Λ polarizations should be very similar.

VI. EXPERIMENTAL CONSIDERATIONS

We collect in this section a series of remarks concerning the feasibility of the types of experiments that are contemplated to measure \mathcal{Q} and \mathcal{P} . Since experiments with the necessary sensitivity have not as yet been performed, our discussion will necessarily be rather general. We will focus particularly on possible backgrounds which may impede the detection of the effects in which we are interested.

Our present-day understanding of measurements

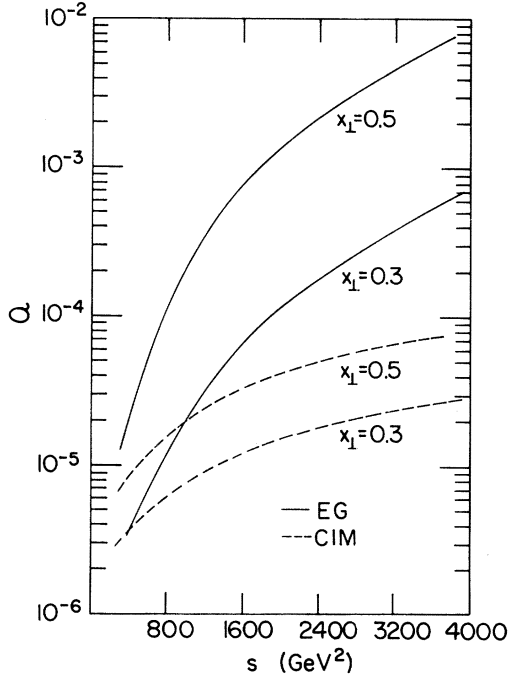


FIG. 4. The weak π^+ asymmetry as a function of s at fixed x_1 and $\theta_{c.m.} = 90^\circ$. The calculations use the LF quark distributions and the CC model of the weak interaction. The CIM results are normalized to agree with those for the EG model at $x_1 = 0.3$ and $s = 400 \text{ GeV}^2$.

of the asymmetry \mathcal{Q} defined in Eq. (1.5) derives primarily from the *total* cross-section measurements for elastic pp scattering⁴² at 15 MeV, and p -Be scattering⁴³ at 6 GeV/c. The measured values,

$$\begin{aligned} \mathcal{Q}(pp) &= (1 \pm 4) \times 10^{-7}, \\ \mathcal{Q}(p\text{-Be}) &= (5 \pm 9) \times 10^{-6}, \end{aligned} \quad (6.1)$$

indicate the level of precision which can be obtained in this class of experiments. The pp experiment is done using a Lamb-shift ion source to produce protons with initial + or - helicity which are scattered from an unpolarized target. The total cross section for each helicity is measured using detectors with $\approx 4\pi$ -sr acceptance. The helicity is flipped at a frequency of 1 kHz so as to minimize possible normalization problems. Errors in such an experiment can arise from a number of sources including the existence of a small transverse component to the proton polarization.

A measurement of \mathcal{Q} in inclusive high-energy π^+ production is substantially more difficult for a number of reasons. To start with, it is difficult to produce a high-energy polarized beam due to depolarizing accelerator resonances.⁴⁴ Secondly, spurious effects can arise from residual transverse components of the initial proton polarization

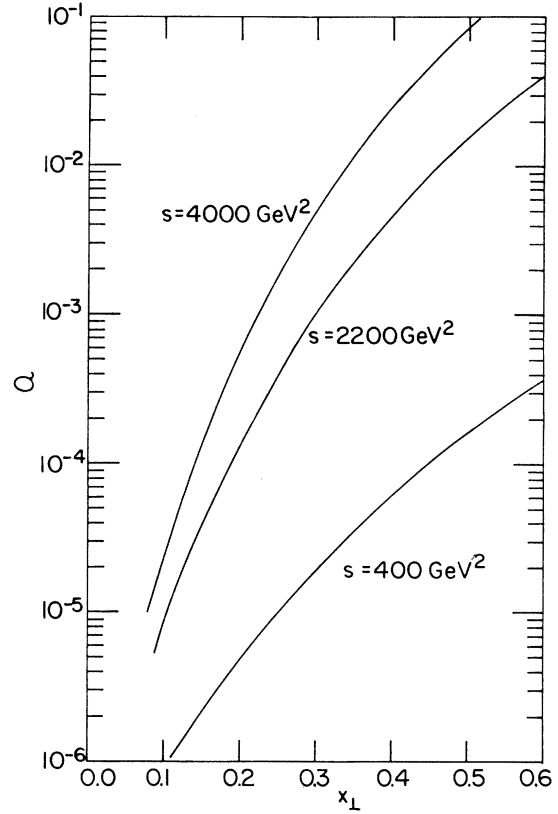


FIG. 5. The weak π^+ asymmetry \mathcal{Q} as a function of x_1 at fixed s and $\theta_{c.m.} = 90^\circ$. The calculations use the LF distribution functions, the EG model of the strong interaction and the AT^+ model of the weak interaction.

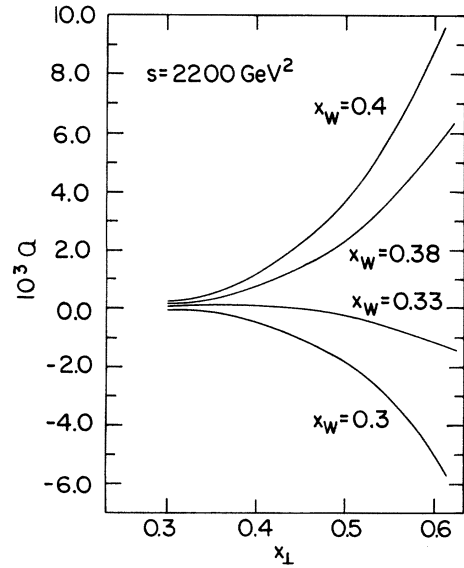


FIG. 6. Demonstration of the sensitivity of $\mathcal{Q}(\pi^+)$ to the value of x_W in the BIM model. The calculations use the EG model of the strong interaction and the LF distribution functions. For $x_W = 0.33$, $\mathcal{Q}(\pi^+)$ vanishes somewhere in the range $0.3 < x_1 < 0.5$.

TABLE III. Invariant cross sections and calculated values of the longitudinal polarization \mathcal{P} for $pp \rightarrow \Lambda X$ at $\theta_{c.m.} = 90^\circ$ and $x_1 = 0.3$ and 0.5 . \mathcal{P} is defined in Eq. (1.6), the strong cross sections are calculated using the EG model, and the weak models are defined in the text.

s (GeV ²)	$E d\sigma/d^3p$ (cm ² c ³ GeV ⁻²)	\mathcal{P} (CC)	AT ⁺ /CC	AT ⁻ /CC	$x_W = \frac{1}{3}$	BIM/CC $x_W = \frac{3}{8}$ $x_W = \frac{2}{5}$	
$x_1 = 0.3$							
400	2.7×10^{-33}	3.3×10^{-5}	2.8	0.3	1.0	1.2	1.3
800	1.0×10^{-34}	1.5×10^{-4}	2.8	0.3	1.0	1.2	1.3
1200	1.3×10^{-35}	4.1×10^{-4}	2.8	0.3	1.0	1.2	1.3
1600	2.9×10^{-36}	8.5×10^{-4}	2.8	0.3	1.0	1.2	1.3
2000	8.6×10^{-37}	1.5×10^{-3}	2.8	0.3	1.0	1.2	1.3
2400	3.2×10^{-37}	2.5×10^{-3}	2.8	0.3	1.0	1.2	1.3
2800	1.3×10^{-37}	3.7×10^{-3}	2.8	0.3	1.0	1.2	1.3
3200	6.3×10^{-38}	5.4×10^{-3}	2.8	0.3	1.0	1.2	1.3
3600	3.2×10^{-38}	7.6×10^{-3}	2.8	0.3	1.0	1.2	1.3
4000	1.8×10^{-38}	9.8×10^{-3}	2.9	0.2	1.0	1.2	1.3
$x_1 = 0.5$							
400	7.2×10^{-37}	2.2×10^{-4}	3.0	-0.04	0.95	1.2	1.3
800	1.8×10^{-38}	1.3×10^{-3}	3.0	-0.04	0.95	1.2	1.3
1200	1.8×10^{-39}	4.1×10^{-3}	3.0	-0.05	0.95	1.2	1.3
1600	3.5×10^{-40}	9.0×10^{-3}	3.0	-0.06	0.95	1.2	1.3
2000	9.6×10^{-41}	1.8×10^{-2}	3.0	-0.06	0.95	1.2	1.3
2400	3.4×10^{-41}	2.8×10^{-2}	3.0	-0.07	0.95	1.2	1.3
2800	1.4×10^{-41}	4.3×10^{-2}	3.0	-0.07	0.95	1.2	1.3
3200	6.6×10^{-42}	6.2×10^{-2}	3.0	-0.08	0.95	1.2	1.3
3600	3.2×10^{-42}	8.9×10^{-2}	3.1	-0.09	0.95	1.2	1.3
4000	1.7×10^{-42}	1.1×10^{-1}	3.1	-0.09	0.96	1.2	1.3

TABLE IV. Invariant cross sections and calculated values of the longitudinal polarization \mathcal{P} for $pp \rightarrow \Lambda X$ at $\theta_{c.m.} = 90^\circ$ and $s = 400, 2200,$ and 4000 GeV². \mathcal{P} is defined in Eq. (1.6), the strong cross sections are calculated using the EG model, and the weak models are defined in the text.

x_1	$E d\sigma/d^3p$ (cm ² c ³ GeV ⁻²)	\mathcal{P} (CC)	AT ⁺ /CC	AT ⁻ /CC	$x_W = \frac{1}{3}$	BIM/CC $x_W = \frac{3}{8}$ $x_W = \frac{2}{5}$	
$s = 400$ GeV ²							
0.1	7.8×10^{-29}	1.5×10^{-6}	2.8	0.60	1.2	1.3	1.4
0.2	2.7×10^{-31}	8.6×10^{-6}	2.8	0.42	1.1	1.2	1.3
0.3	2.7×10^{-33}	3.3×10^{-5}	2.8	0.30	1.0	1.2	1.3
0.4	4.1×10^{-35}	9.5×10^{-5}	2.9	0.11	1.0	1.2	1.3
0.5	7.2×10^{-37}	2.2×10^{-4}	3.0	-0.04	0.95	1.2	1.3
0.6	1.1×10^{-38}	4.4×10^{-4}	3.0	-0.19	0.91	1.2	1.3
$s = 2200$ GeV ²							
0.1	2.3×10^{-32}	1.8×10^{-5}	2.9	0.65	1.2	1.3	1.4
0.2	1.4×10^{-34}	2.8×10^{-4}	2.9	0.45	1.1	1.3	1.3
0.3	5.1×10^{-37}	2.0×10^{-3}	2.9	0.27	1.1	1.2	1.3
0.4	4.4×10^{-39}	7.4×10^{-3}	3.0	0.11	0.98	1.2	1.3
0.5	5.6×10^{-41}	2.2×10^{-2}	3.0	-0.06	0.94	1.2	1.3
0.6	7.2×10^{-43}	4.8×10^{-2}	3.1	-0.22	0.92	1.2	1.3
$s = 4000$ GeV ²							
0.1	1.9×10^{-32}	5.5×10^{-4}	2.9	0.65	1.2	1.3	1.4
0.2	6.4×10^{-36}	1.2×10^{-3}	2.9	0.45	1.1	1.3	1.3
0.3	1.8×10^{-38}	9.8×10^{-3}	2.9	0.24	1.0	1.2	1.3
0.4	1.4×10^{-40}	4.1×10^{-2}	3.0	0.09	0.98	1.2	1.3
0.5	1.7×10^{-42}	1.1×10^{-1}	3.1	-0.09	0.96	1.2	1.3
0.6	2.1×10^{-44}	2.5×10^{-1}	3.1	-0.25	0.92	1.2	1.3

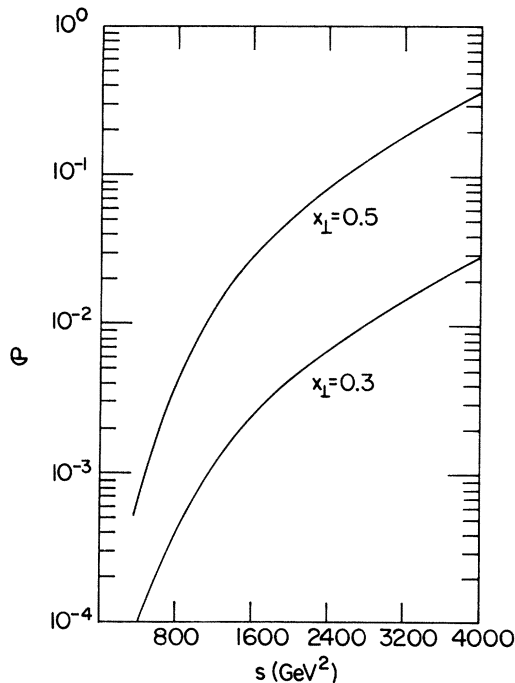


FIG. 7. The longitudinal polarization of an inclusively produced Λ as a function of s at fixed x_{\perp} and $\theta_{c.m.} = 90^\circ$. The calculations use the EG model of the strong interaction and the AT⁺ model of the weak interaction.

which are known to produce large asymmetries⁴⁵ in inclusive π production. Thirdly, a nonzero value of $\mathcal{G}(\pi)$ can result from the *strong* production of some hadron h which then decays weakly. An example would be the contribution to $\mathcal{G}(\pi^+)$ resulting from the strong production $pp \rightarrow \Lambda X$ followed by the weak pv decay $\Lambda \rightarrow p\pi^-$. It is easy to see that if some of the polarization of the initial p is transmitted to the outgoing Λ via the strong production mechanism then a contribution to $\mathcal{G}(\pi^+)$ will result from the circumstance that, as a consequence of parity violation in the $\Lambda \rightarrow p\pi^-$ decay, more pions are emitted in the direction of the Λ spin than against it. This background is minimized for inclusive π^+ production (compared to π^- or π^0) for the following reasons: (a) There is no background from the strong production of Λ^0 , Σ^0 , Σ^- , Ξ^0 , Ξ^- , or Ω^- since none of these particles decays to form a π^+ . (b) π^+ can arise from $\Sigma^+ \rightarrow n\pi^+$ but this decay is very nearly parity conserving,⁴⁶

$$\alpha(\Sigma^+ \rightarrow n\pi^+) = 0.066 \pm 0.016, \quad (6.2)$$

where $\alpha(\Sigma^+ \rightarrow n\pi^+)$ is the usual pv parameter describing the *SP* interference term in nonleptonic hyperon decay. Weak decays of charmed baryons can also contribute to $\mathcal{G}(\pi^+)$. Since the production of charmed baryons is expected to be smaller than

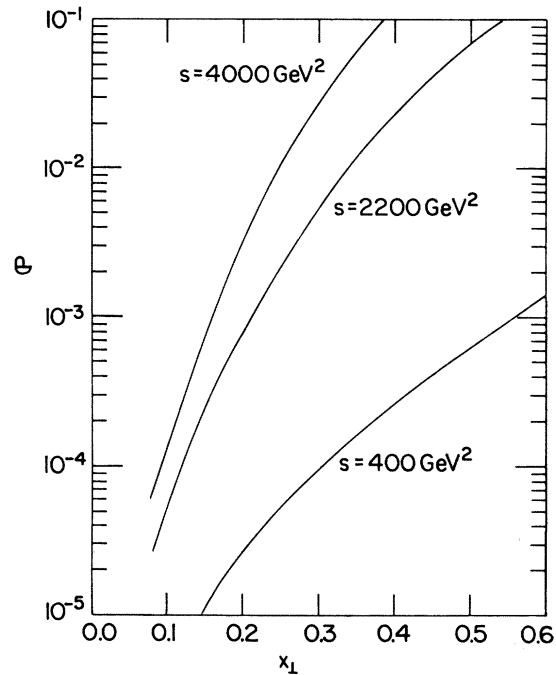


FIG. 8. The longitudinal polarization of an inclusively produced Λ as a function of x_{\perp} at fixed s and $\theta_{c.m.} = 90^\circ$. The calculations use the EG model of the strong interaction and the AT⁺ model of the weak interaction.

that of ordinary hyperons, the charmed contribution to $\mathcal{G}(\pi^+)$ is likely to be suppressed compared to that from Σ^+ decay, but detailed numerical estimates will have to await additional experimental information on charm production.

Turning to $\mathcal{P}(\Lambda)$ we begin by noting that pv effects in the high-energy inclusive process $p + \text{Be} \rightarrow \Lambda X$ have been looked for recently.⁴⁷ In this experiment the pv decay $\Lambda \rightarrow p\pi^-$ is used to determine the polarization vector \vec{P} of the outgoing Λ which is produced by incident unpolarized 300-GeV protons. For the pv parameter αP_y , where $\alpha = \alpha(\Lambda \rightarrow p\pi^-) = 0.647 \pm 0.013$ is the same parameter discussed above, they find

$$\alpha P_y = -0.009 \pm 0.003. \quad (6.3)$$

Inherently measurements of $\mathcal{P}(\Lambda)$ appear to have fewer background problems than those of $\mathcal{G}(\pi^+)$, although the corresponding sensitivities may also be lower due in part to reduced statistics. From a theoretical point of view $\mathcal{G}(\pi^+)$ is a somewhat more interesting parameter than $\mathcal{P}(\Lambda)$ since the polarized distribution functions needed to calculate $\mathcal{G}(\pi^+)$ can in principle be extracted from electromagnetic experiments,^{38,48} whereas we have as yet no handle on the distribution functions describing the decay of a polarized quark into a polarized Λ which we need to calculate $\mathcal{P}(\Lambda)$ unambiguously.

VII. CONCLUSIONS

We have motivated the study of weak pv effects in high- p_1 hadron-hadron collisions as a means of probing the parton-parton interaction. The characteristic feature of the parton model which makes such a study useful is that, because of the coherence of the strong and weak interactions at the parton level, the same parton distribution and decay functions describe the strong and weak inclusive processes $hh' \rightarrow cX$. This "commonality" of the distribution and decay functions makes it possible for a study of weak effects to lead to a significant increase in the amount of information available to us, without at the same time incurring a commensurate increase in the number of unknowns.

A related consequence of this "commonality" is that in principle most of the information needed to calculate pv effects in inclusive hadron-hadron scattering can be determined independently from other experiments. As noted previously, the distribution of quarks within a polarized proton can be determined from ep experiments.^{38,48} Information about the weak coupling of quarks (although not direct information about weak qq scattering) can be extracted from semileptonic weak processes. Information about the strong interaction can be obtained not only from single-particle inclusive data, but from measurements of multiparticle final states and exclusive processes as well. The important role that weak measurements at high p_1 can play is derived from the fact that all of these parts come together in a single system. As a result one can use knowledge of one portion of the system to explore properties of a second portion. As was demonstrated in Sec. V, if one varies one segment of the calculation—such as the assumed form of the neutral weak current—while holding all other parts fixed (strong model, distributions, etc.) the predicted weak effects can be quite different. Consequently the possibility of distinguishing among different models of these processes exists in the measurement of high- p_1 phenomena.

It is also clear from our analysis that there are combinations of models (and it is particularly true for the choice of phases) which will produce vanishingly small effects over at least some range of x_1 . For example, the use of the AT⁻ model of the weak interaction in the calculation of $\mathcal{O}(\Lambda)$ led to a zero in $\mathcal{O}(\Lambda)$ between $x_1 = 0.4$ and $x_1 = 0.5$. Consequently, if a model such as this one were to truly represent the real physical world, it would be necessary to measure \mathcal{O} over a large range of x_1 in order to establish its existence and behavior. Hence the measurement of a small longitudinal polarization is not necessarily an indication that parity violation is not present at the fundamental

quark-quark level.

Throughout our calculations we have assumed that the strong quark-quark-gluon coupling is pure V , while the weak quark-quark interaction is some combination of V and A . Only the CC weak interaction is known for certain to be V,A and hence it is possible that the strong and/or NC weak quark-quark interaction might actually involve the S, P, T covariants. Since a V,A quark-quark coupling preserves the helicity of the incoming quark, whereas any combination of S, P, T flips the helicity, an amplitude which is S, P, T cannot interfere coherently with one which is V,A . It follows that if the EG amplitude (or the strong quark-quark interaction more generally) actually originated from S, P, T , while the weak NC was V,A as expected, then there would be no weak-strong interference effects at all, and hence \mathcal{G} and \mathcal{O} would be too small to be measured by any foreseeable technique. On the other hand, if the strong amplitude is vectorial, whereas the weak NC is some combination of S, P, T ,^{29,49} then the strong interaction would still be coherent with the CC weak interaction. Thus a study of weak effects in high- p_1 inclusive scattering could elucidate the space-time structure of the strong and NC weak interactions.

Setting aside the possibility of S, P, T couplings it is clear that, despite uncertainties in our calculations, an increase in weak effects at large p_1 in inclusive processes is a general feature of constituent models. In addition, the functional form of \mathcal{G} and \mathcal{O} can be quite sensitive to the details of the input parameters so that there is potentially a great deal that can be learned from their measurement.

Because of the small size of the invariant cross sections, the experimental detection of weak effects at large p_1 will be difficult, even if these effects turn out to be equal to the largest values which are predicted here. Nevertheless, there are many interesting questions which can be explored uniquely through such experiments, such as the form of the weak parton-parton interaction. Indeed one can justify the need for a study of weak effects at high p_1 more strongly by noting that, as difficult as the proposed experiments are, they represent the only way of *directly* studying the weak $\Delta S = 0$ parton-parton interaction. The situation here is thus completely analogous to that encountered in studying the weak $\Delta S = 0$ hadron-hadron interaction, which study requires difficult experiments on parity violation in nuclei.³²

APPENDIX

The basic structure of the models used to describe the production of particles with large p_1 in high-energy hadron-hadron collisions was first de-

veloped by Berman, Bjorken, and Kogut¹⁹ (BBK) and utilizes the parton-model ideas which have proved successful in describing deep-inelastic electroproduction data. The model describes the production as occurring in three steps, as pictured in Fig. 1. The incident hadrons first fragment into their basic constituents (called partons), which then scatter through large angles. Finally, one of the scattered partons "decays" into the observed particle.

The incident particles are said to fragment in the sense that the constituents behave as free particles during the scattering. This picture of free partons scattering incoherently is found to provide an accurate description of electroproduction.⁴ The connection between the incident hadron and the parton system is made by assuming that the partons all move in the direction of the incident particle and then defining the function $u_i(x)dx$, which represents the total number of partons of type i which carry a fraction $x(0 \leq x \leq 1)$ of the momentum of the incident particle. The particular form of these functions will, of course, depend upon both the nature of the incident particle and upon the nature of the constituents.

In the limit of high energies and high-momentum transfers we assume that all hadron and parton masses may be ignored. Hence, following BBK, we introduce the scaling variables (see Fig. 1)

$$\hat{x}_1 = -\frac{(p_i - p_k)^2}{(p_i + p_j)^2} = -\frac{\hat{u}}{\hat{s}}$$

and

$$\hat{x}_2 = -\frac{(p_i - p_k)^2}{(p_i + p_j)^2} = -\frac{\hat{t}}{\hat{s}}, \quad (\text{A1})$$

and note that

$$\hat{x}_1 + \hat{x}_2 = \frac{-(\hat{u} + \hat{t})}{\hat{s}} = 1. \quad (\text{A2})$$

The differential cross section for parton-parton scattering can thus be written in the form

$$d\hat{\sigma} = f(\hat{x}_1, \hat{x}_2, \hat{s}) \delta(\hat{x}_1 + \hat{x}_2 - 1) d\hat{x}_1 d\hat{x}_2. \quad (\text{A3})$$

If the scattered partons are both quarks, so that neither can be observed directly, then the hadron which is actually observed can result from the decay of either of the scattered quarks. Assuming that the observed particle comes from the decay of a parton with momentum p_k , as indicated in Fig. 1, we must include in the calculation of the production of particle c terms corresponding to the cases where either parton i or parton j is scattered into

the momentum state p_k . As indicated in Fig. 2, this can be done by including terms corresponding to both \hat{t} - and \hat{u} -channel exchange in the quark-quark scattering process. Thus it is convenient to introduce a second cross section $d\hat{\sigma}'$ defined by

$$\begin{aligned} d\hat{\sigma}'(p_i, p_k) &= d\hat{\sigma}(p_k, p_i) \\ &= f'(\hat{x}_1, \hat{x}_2, \hat{s}) \delta(\hat{x}_1 + \hat{x}_2 - 1) d\hat{x}_1 d\hat{x}_2. \end{aligned} \quad (\text{A4})$$

$d\hat{\sigma}$ and $d\hat{\sigma}'$ thus represent the parton-parton differential cross sections in the \hat{t} and \hat{u} channels, respectively. Furthermore, if the scattered partons are identical, a term corresponding to the interference of the \hat{t} and \hat{u} channels must be included,

$$\begin{aligned} d\hat{\sigma}^{\text{idem}} &= d\hat{\sigma} + d\hat{\sigma}' \\ &+ f''(\hat{x}_1, \hat{x}_2, \hat{s}) \delta(\hat{x}_1 + \hat{x}_2 - 1) d\hat{x}_1 d\hat{x}_2. \end{aligned} \quad (\text{A5})$$

These terms will be included when we write the cross section for $hh' \rightarrow cX$, where h and h' are hadrons.

In describing the decay of the scattered partons into the observed particles, it is assumed that the final-state interactions are typical strong interactions, and in particular that they do not involve large momentum transfer processes. Hence the particles which emerge from the decay are expected to appear as a jet of particles traveling in the direction of the scattered parton with a dispersion in momentum transverse to the parton momentum of ~ 300 MeV/ c . A specific mechanism which has been suggested for the decay is for the scattered parton to communicate with the "wee" partons of the originally incident particles (those partons with $x \ll 1$) through a cascade emission of parton-antiparton pairs.^{19,50} In practice one defines the functions $G_{i/c}(z)$ such that the differential probability of finding a hadron c emerging from the decay of a scattered parton i with fraction z of the parton's four-momentum is

$$dP_{i/c}(z) = \frac{G_{i/c}(z)}{z} dz. \quad (\text{A6})$$

From conservation of energy $G_{i/c}(z)$ obeys the sum rule

$$\sum_c \int G_{i/c}(z) dz = 1 \quad (\text{A7})$$

independent of the type of parton.¹⁹

Having defined the quantities needed to describe the scattering $hh' \rightarrow cX$, we may write down the expression for the differential scattering cross section:

$$d\sigma = \sum_{ij} \int [u_i(x_i) dx_i] [u_j(x_j) dx_j] \left[d\hat{\sigma}_{(i \neq j)}(p_k, p_l) \frac{G_{i/c}(x)}{x} + d\hat{\sigma}_{(i \neq j)}(p_l, p_k) \frac{G_{j/c}(x)}{x} + \delta_{ij} d\hat{\sigma}_{ij}^{\text{idem}} \frac{G_{i/c}(x)}{x} dx \right] \quad (\text{A8a})$$

or

$$d\sigma = \sum_{ij} \int u_i(x_i) u_j(x_j) \{ f_{ij}(\hat{x}_1, \hat{x}_2, \hat{s}) G_{i/c}(x) + f'_{ij}(\hat{x}_1, \hat{x}_2, \hat{s}) G_{j/c}(x) + \delta_{ij} f''(\hat{x}_1, \hat{x}_2, \hat{s}) G_{i/c}(x) \} x^{-1} \delta(\hat{x}_1 + \hat{x}_2 - 1) dx_i dx_j d\hat{x}_1 d\hat{x}_2 dx. \quad (\text{A8b})$$

The variables x_i , x_j , and x are defined in Fig. 1. The summation over i and j in Eq. (A8) sums incoherently over the scattering of all constituents of the incident particles, and the integration is over all possible internal kinematic configurations which can lead to the same final state for particle c . As commented upon above, the first two terms are included to take into account the fact that either of the scattered partons may decay to form the observed hadron c , and the third term is needed when the scattered partons are identical.

Equation (A8) for the scattering cross section may be simplified by introducing variables x_1 and x_2 which are defined in analogy with the variables \hat{x}_1 and \hat{x}_2 of Eq. (A1). Here we define

$$x_1 = -(p_b - p_c)^2 / (p_a + p_b)^2 = -u/s, \quad (\text{A9})$$

$$x_2 = -(p_a - p_c)^2 / (p_a + p_b)^2 = -t/s.$$

Since the process $hh' \rightarrow cX$ is, in general, highly inelastic ($E_c \neq E_h$ in the center-of-momentum frame), Eq. (A2) is replaced—for the observed process—by the condition

$$x_1 + x_2 \leq 1. \quad (\text{A10})$$

The connection between the parton-parton variables and the variables of the observed $hh' \rightarrow cX$ process can be determined by using the definitions given above and in Fig. 1. Recalling that the mass-

$$E_c \frac{d\sigma}{d^3p_c} = \frac{1}{\pi s} \frac{d\sigma}{dx_1 dx_2} = \frac{1}{\pi s} \sum_{ij} \int \frac{dx_i dx_j}{x^2 (xx_i - x_1)} u_i(x_i) u_j\left(\frac{x_i x_2}{xx_i - x_1}\right) [f(x_1, x_2, s; x_i, x) G_{i/c}(x) + f'(x_1, x_2, s; x_i, x) G_{j/c}(x) + \delta_{ij} f''(x_1, x_2, s; x_i, x) G_{i/c}(x)]. \quad (\text{A15})$$

The limits of integration on the variables x_i and x may be determined through the condition that the arguments of the functions u_i , u_j , and $G_{i/c}$ lie between zero and one,

$$0 \leq x_i \leq 1 \quad (\text{A16a})$$

$$0 \leq x_j = \frac{x_i x_2}{xx_i - x_1} \leq 1 \quad (\text{A16b})$$

$$0 \leq x \leq 1. \quad (\text{A16c})$$

The inequalities of Eq. (A16) require

$$\frac{x_1}{x - x_2} \leq x_i \leq 1 \text{ and } x_1 + x_2 \leq x \leq 1, \quad (\text{A17a})$$

es of the hadrons and of the quarks are assumed to be negligible, we have

$$\hat{x}_1 = -[x_j p_b - (1/x) p_c]^2 / (x_i p_a + x_j p_b)^2 = \frac{(x_j/x) p_b \cdot p_c}{x_i x_j p_a \cdot p_b} = \frac{x_1}{xx_i}, \quad (\text{A11a})$$

$$\hat{x}_2 = -[x_i p_a - (1/x) p_c]^2 / (x_i p_a + x_j p_b)^2 = \frac{(x_i/x) p_a \cdot p_c}{x_i x_j p_a \cdot p_b} = \frac{x_2}{xx_j}, \quad (\text{A11b})$$

and $\hat{x}_1 + \hat{x}_2 = 1$ implies

$$x_j = \frac{x_i x_2}{xx_i - x_1}. \quad (\text{A12})$$

Hence we may write the variables (x_i, x, \hat{x}_1, x_j) in terms of the variables (x_i, x, x_1, x_2) ,

$$x_i = x_i, \quad \hat{x}_1 = \frac{x_1}{xx_i}, \quad (\text{A13})$$

$$x = x, \quad x_j = \frac{x_i x_2}{xx_i - x_1},$$

and the integral of Eq. (A8) may be transformed into the variables (x_i, x, x_1, x_2) through the Jacobian

$$\left| \frac{\partial(x_i, x, x_1, x_j)}{\partial(x_i, x, x_1, x_2)} \right| = \frac{1}{x(xx_i - x_1)}. \quad (\text{A14})$$

The differential cross section thus becomes

or

$$x_2 + \frac{x_1}{x_i} \leq x \leq 1 \text{ and } \frac{x_1}{1 - x_2} \leq x_i \leq 1. \quad (\text{A17b})$$

In order to calculate the invariant cross section for a particular scattering process we must, of course, specify the nature of the constituents of the incident particles, the parton-parton scattering mechanism, and which of the scattered constituents can decay to form the observed particle. A number of models based on the above mechanism have been developed which can differ significantly in their description of these processes. Among these the FF²⁵ and EG²⁰ models appear to be most easily

capable of accounting for the recent data on inclusive single-particle and jet production.⁵¹ Notwithstanding the successes of these models, there are a number of questions which must be more fully addressed before any final conclusions can be drawn about their viability. For the EG model these include understanding the magnitude of the gluon coupling α_s and the question of the color transformation properties of the gluon. For the FF

model the description of inclusive baryon production remains an open problem. Both models have yet to deal with elastic scattering, as well as with the question of the physical interpretation of the respective phenomenological quark-quark cross sections. The interested reader can find a discussion of some of these points in the original exposition of the FF²⁵ and EG²⁰ models and in some more recent work by various authors.^{21,52-54}

*Work supported in part by the U. S. Energy Research and Development Administration.

†Present address: Theoretical Division, Sandia Laboratories, Livermore, Ca. 94550.

¹R. H. Dalitz, in *Baryon Resonances — 73*, Proceedings of the Purdue Conference, edited by E. C. Fowler (Purdue Univ. Press, West Lafayette, Indiana, 1973), p. 393; J. J. J. Kokkedee, *The Quark Model* (Benjamin, Reading, Mass., 1969); H. J. Lipkin, Phys. Rep. 8C, 173 (1973).

²T. Appelquist, A. De Rújula, H. D. Politzer, and S. L. Glashow, Phys. Rev. Lett. 34, 365 (1975); E. Eichten, K. Gottfried, T. Kinoshita, J. Kogut, K. D. Lane, and T.-M. Yan, *ibid.* 34, 369 (1975).

³F. J. Gilman, in *Proceedings of the XVII International Conference on High Energy Physics, London, 1974*, edited by J. R. Smith (Rutherford Laboratory, Chilton, Didcot, Berkshire, England, 1974), p. IV-149.

⁴R. P. Feynman, *Photon-Hadron Interactions* (Benjamin, Reading, Mass., 1972).

⁵L. Van Hove, Phys. Rep. 1C, 347 (1971).

⁶U. Amaldi, R. Biancastelli, C. Bosio, G. Matthiae, J. V. Allaby, W. Bartel, G. Cocconi, A. N. Diddens, R. W. Dobinson, V. Elings, L. Litt, L. S. Rochester, and A. M. Wetherell, Phys. Lett. 36B, 504 (1971).

⁷K. Imaeda, Nuovo Cimento 48A, 482 (1967).

⁸E. Fischbach and G. W. Look, Phys. Rev. D 13, 752 (1976).

⁹E. Fischbach and G. W. Look, in *High Energy Physics with Polarized Beams and Targets*, proceedings of the Argonne Conference, 1976, edited by M. L. Marshak (AIP, New York, 1976), p. 258.

¹⁰E. M. Henley, in Proceedings of the Summer Studies on High-Energy Physics with Polarized Beams, Argonne, 1974, Report No. ANL/HEP 75-02, p. XII-1.

¹¹E. M. Henley and F. R. Krejs, Phys. Rev. D 11, 605 (1975).

¹²L. L. Frankfurt and V. B. Kopeliovich, Nucl. Phys. B103, 360 (1976).

¹³L. L. Frankfurt, Zh. Eksp. Teor. Fiz. Pis'ma Red. 12, 536 (1970) [JETP Lett. 12, 379 (1970)]; Zh. Eksp. Teor. Fiz. 61, 45 (1975) [Sov. Phys. — JETP 34, 23 (1972)].

¹⁴M. Dobovoy, P. Langacker, and M. Suzuki, Phys. Rev. D 4, 1474 (1971).

¹⁵N. N. Nikolaev, Yad. Fiz. 17, 119 (1973) [Sov. J. Nucl. Phys. 17, 62 (1973)].

¹⁶K. H. Craig, Nucl. Phys. B109, 156 (1976).

¹⁷J. Missimer, L. Wolfenstein, and J. Gunion, Nucl. Phys. B111, 20 (1976).

¹⁸F. Halzen, Phys. Rev. D 15, 1929 (1977).

¹⁹S. M. Berman, J. D. Bjorken, and J. B. Kogut, Phys. Rev. D 4, 3388 (1971).

²⁰E. Fischbach and G. W. Look, Phys. Rev. D 15, 2576 (1977).

²¹G. W. Look and E. Fischbach, Phys. Rev. D 16, 1369 (1977).

²²S. D. Ellis and M. B. Kislinger, Phys. Rev. D 9, 2027 (1974).

²³R. Blankenbecler, S. J. Brodsky, and J. Gunion, Phys. Rev. D 12, 3469 (1975); R. Blankenbecler, S. J. Brodsky, J. F. Gunion, and R. Savit, *ibid.* 10, 2153 (1974).

²⁴D. Sivers, S. J. Brodsky, and R. Blankenbecler, Phys. Rep. 23C, 1 (1976).

²⁵R. D. Field and R. P. Feynman, Phys. Rev. D 15, 2590 (1977).

²⁶The quark distribution functions used in the EG model (Refs. 9, 20, and 21) are those of R. McElhaney and S. F. Tuan, Phys. Rev. D 8, 2267 (1973); Nucl. Phys. B72, 487 (1974).

²⁷E. Fischbach, M. M. Nieto, H. Primakoff, C. K. Scott, and J. Smith, Phys. Rev. Lett. 27, 1403 (1971); J. C. Hardy and I. S. Towner, Nucl. Phys. A254, 221 (1975).

²⁸A. M. Sachs and A. Sirlin, *Muon Physics*, edited by V. W. Hughes and C. S. Wu (Academic, New York, 1975), Vol. II.

²⁹E. Fischbach, J. T. Gruenwald, S. P. Rosen, H. M. Spivack, and B. Kayser, Phys. Rev. Lett. 37, 582 (1976); Phys. Rev. D 15, 97 (1977).

³⁰F. Sciulli, in *Particles and Fields — 1975*, Proceedings of the Meeting of the Division of Particles and Fields of the APS, Seattle, edited by H. Lubatti and P. M. Mockett (Univ. of Washington, Seattle, 1975), p. 76.

³¹B. Aubert, A. Benvenuti, D. Cline, W. T. Ford, R. Imlay, T. Y. Ling, A. K. Mann, F. Messing, J. Pilcher, D. D. Reeder, C. Rubbia, R. Stefanski, and L. Sulak, Phys. Rev. Lett. 33, 984 (1974).

³²E. Fischbach and D. Tadić, Phys. Rep. 6C, 123 (1973).

³³S. L. Adler and S. F. Tuan, Phys. Rev. D 11, 129 (1975).

³⁴S. L. Glashow, J. Iliopoulos, and L. Maiani, Phys. Rev. D 2, 1285 (1970); B. J. Bjorken and S. L. Glashow, Phys. Lett. 11, 255 (1964).

³⁵C. Bouchiat, J. Iliopoulos, and P. Meyer, Phys. Lett. 38B, 519 (1972); M. A. B. Bég and A. Sirlin, Annu. Rev. Nucl. Sci. 24, 379 (1974).

³⁶A. Salam and J. C. Ward, Phys. Lett. 13, 168 (1964); S. Weinberg, Phys. Rev. Lett. 19, 1264 (1967).

³⁷B. W. Lee, summary talk at International Neutrino Conference, 1976, Aachen, W. Germany (unpublished).

- ³⁸G. W. Look and E. Fischbach, *Phys. Rev. D* **16**, 211 (1977).
- ³⁹J. Kuti and V. F. Weisskopf, *Phys. Rev. D* **4**, 3418 (1971).
- ⁴⁰L. M. Sehgal, *Phys. Rev. D* **10**, 1663 (1974).
- ⁴¹F. W. Büsler, L. Camilleri, L. DiLella, B. G. Pope, A. M. Smith, B. J. Blumenfeld, S. N. White, A. F. Rothenberg, S. L. Segler, M. J. Tannenbaum, M. Banner, J. B. Chèze, H. Kasha, J. P. Pansart, G. Smadja, J. Teiger, H. Zaccone, and A. Zylberstejn, *Phys. Lett.* **61B**, 309 (1976).
- ⁴²J. M. Potter, J. D. Bowman, C. F. Hwang, J. L. McKibben, R. E. Mischke, D. E. Nagle, P. G. Debrunner, H. Frauenfelder, and L. B. Sorensen, *Phys. Rev. Lett.* **33**, 1307 (1974).
- ⁴³J. D. Bowman, C. M. Hoffman, C. F. Hwang, R. E. Mischke, D. E. Nagle, J. M. Potter, D. M. Alde, P. G. Debrunner, H. Frauenfelder, L. B. Sorensen, H. L. Anderson, and R. Talaga, *Phys. Rev. Lett.* **34**, 1184 (1975).
- ⁴⁴Y. Cho, R. L. Martin, E. F. Parker, C. W. Potts, L. G. Ratner, J. Gareyte, C. Johnson, P. Lefèvre, D. Möhl, and A. D. Krisch, in *High Energy Physics with Polarized Beams and Targets*, Proceedings of the Argonne Conference, 1976, edited by M. L. Marshak (AIP, New York, 1976), p. 396; M. Bell, P. Germain, W. Hardt, W. Kubischta, P. Lefèvre, and D. Möhl, *ibid.* p. 405; A. Turrin, *ibid.* p. 414.
- ⁴⁵R. D. Klem, J. E. Bowers, H. W. Courant, H. Kagan, M. L. Marshak, E. A. Peterson, K. Ruddick, W. H. Dragoset, Jr., and J. B. Roberts, *Phys. Rev. Lett.* **36**, 929 (1976).
- ⁴⁶Particle Data Group, *Rev. Mod. Phys.* **48**, S1 (1976).
- ⁴⁷G. Bunce, R. Handler, R. March, P. Martin, L. Pondrom, M. Sheaff, K. Heller, O. Overseth, P. Skubic, T. Devlin, B. Edelman, R. Edwards, J. Norem, L. Schachinger, and P. Yamin, *Phys. Rev. Lett.* **36**, 1113 (1976).
- ⁴⁸M. J. Alguard, W. W. Ash, G. Baum, J. E. Clendenin, P. S. Cooper, D. H. Coward, R. D. Ehrlich, A. Etkin, V. W. Hughes, H. Kobayakawa, K. Kondo, M. S. Lubell, R. H. Miller, D. A. Palmer, W. Raith, N. Sasao, K. P. Schüler, D. J. Sherden, C. K. Sinclair, and P. A. Souder, *Phys. Rev. Lett.* **37**, 1258 (1976); **37**, 1261 (1976).
- ⁴⁹B. Kayser, G. T. Garvey, E. Fischbach, and S. P. Rosen, *Phys. Lett.* **52B**, 385 (1974).
- ⁵⁰G. R. Farrar and J. L. Rosner, *Phys. Rev. D* **10**, 2226 (1974) and references cited therein.
- ⁵¹C. Bromberg, G. Fox, R. Gomez, J. Pine, S. Stampke, K. Yung, S. Erhan, E. Lorenz, M. Medinnis, J. Rohlf, P. Schlein, V. Ashford, H. Haggerty, R. Juhala, E. Malamud, S. Mori, R. Abrams, R. Delzennero, H. Goldberg, S. Margulies, D. McLeod, J. Solomon, R. Stanek, A. Dzierba, and W. Kropac, *Phys. Rev. Lett.* **38**, 1447 (1977).
- ⁵²E. Fischbach and G. W. Look, *Phys. Rev. D* **16**, 1571 (1977).
- ⁵³R. Cutler and D. Sivers, *Phys. Rev. D* **16**, 679 (1977).
- ⁵⁴S. D. Ellis and R. Stroynowski, SLAC Report No. 1903, 1977 (unpublished).